Green closed-loop cathode regeneration from spent NMC-based lithium-ion batteries through bioleaching

Minh Phuong Do [#] [†,‡], Joseph Jegan Roy [#] [†,‖,‡], Bin Cao * [‖,§], Madhavi Srinivasan [†, ‡]**

[†] Energy Research Institute @ NTU (ERI@N), SCARCE Laboratory, Nanyang Technological University, 62 Nanyang Dr, Singapore 637459

[‖] Singapore Centre for Environmental Life Sciences Engineering, Nanyang Technological University, 60 Nanyang Dr, Singapore 637551

[‡] School of Materials Science and Engineering, Nanyang Technological University, 50 Nanyang Avenue, Singapore 639798

[§] School of Civil and Environmental Engineering, Nanyang Technological University, 50 Nanyang Avenue, Singapore 639798

[#] These author has equally contributed to this work

* Corresponding Author

Contact: Madhavi@ntu.edu.sg Tel.: +65 67904606
BinCao@ntu.edu.sg Tel.: +65 67905277
jeganroy@ntu.edu.sg
minhphuong.do@ntu.edu.sg

Abstract

Addressing the growing volume of end-of-life lithium-ion battery (LIB) waste is one of the global challenges in tackling the electronic waste problem. In this study, the regeneration of $LiNi_{0.3}Co_{0.3}Mn_{0.3}O_2$ (NMC_{111}) and $LiNi_{0.6}Co_{0.2}Mn_{0.2}O_2$ (NMC_{622}) cathode active materials from end-of-life LIBs was accomplished through an environmentally friendly bioleaching process. In the bioleaching process mediated by *Acidithiobacillus ferrooxidans*, 85.5% of Ni, 91.8% of Mn, 90.4% of Co, and 89.9% of Li were leached out from NMC-based spent LIBs in 6 h at a pulp density of 100 g/L. One of the challenges in bioleaching-based metal recovery is the presence of impurities, including Cu, Al and Fe (excess Fe^{3+} and Fe^{2+} from bacterial nutrients). The impurity removal was performed by air oxidation and pH adjustment without

substantial losses of other metallic ions. Thereafter, ammonium oxalate coprecipitation effectively recovered the transition metal ions as metal oxalates from the bioleaching liquor. NMC_{111} and NMC_{622} were regenerated from the coprecipitated product. The electrochemical stability of the regenerated NMC_{111} and NMC_{622} was comparable to commercial NMC (~85% of capacity retention after 50 cycles at 100 mA g^{-1}). This regeneration approach appears promising in LIBs recycling for long-term industrial development.

Keywords: Lithium-ion batteries, Bioleaching, *Acidithiobacillus ferrooxidans*, Impurities removal, Cathode regeneration

Introduction

The development of sustainable energy sources and storage solutions has been pushed by ever-increasing global energy requirements as well as environmental destruction. Lithium-ion batteries (LIBs) have been widely used as secondary energy storage in consumer electronics, electric vehicles, and power grid systems due to high energy density, high power density, long lifespan, and compact size. LIBs have a global market capitalization of USD 40 billion and are expected to grow to USD 139.36 billion by 2026 [1]. The rising demand for electric vehicles (EVs) needs a massive number of LIB packs, which is expected to reach 1 million by 2030 [2]. As a result, the output of discarded LIBs is estimated to rise from 10,700 tons in 2012 to 464,000 tons in 2025, representing a 59% growth rate every year[3]. Because of the massive use of LIBs in electronic devices, electric vehicles (EVs), and energy storage, metal recovery from spent LIBs has a higher resource benefit, reduces the usage of pure metals in energy storage, and offers environmental protection [2, 4-6]. In the long-term, recovery of valuable material from spent LIBs is efficacious in alleviating the shortage of purified minerals and reducing the manufacturing price. [6-8]. In addition, LIB recycling also contributes to reducing metal contamination into the water stream and soil, cutting CO_2 emissions, and supporting a more sustainable circular economy [6, 9].

Currently, pyrometallurgy and acid-based hydrometallurgy are the most popular approaches used to recover valuable metals from spent LIBs [5, 10, 11 12]. Cobalt, nickel, and copper are generally recovered as slag in pyrometallurgy by melting spent LIBs at high temperatures (500–1000 °C); however, lithium vanished as gas cannot be recovered [13]. The pyrometallurgical process consumes much energy, has a high capital cost, and generates many noxious gases. On the other hand, in the conventional hydrometallurgical process, metals are typically leached out by mineral acids as leaching agents, such as H_2SO_4, HNO_3, HCl, aided with oxidant (e.g. H_2O_2), which involves additional disposal investment [14, 15]. As metals are soluble in acid solutions, the hydrometallurgical process has a better recovery efficiency than the pyrometallurgical process. However, the hydrometallurgical process has some drawbacks, including complex operating steps, production of a significant amount of acid wastes, and the emission of toxic gases such as Cl_2, SO_3, and NO_x, The acid wastes and toxic gases emission are harmful to human health and the environment. The treatment of acid wastes and gases emission incurs additional costs. New approaches, such as Ferro-chemistry based recycling [16], gradient and facile extraction [17], based on the leaching kinetics of cathode material [18] and sequential extraction of metals using organic and mineral acids [19], has been explored in the hydrometallurgical process. Toward green chemistry regulations, organic acids such as oxalic acid, malic acid, acetic acid, tartaric acid, and citrus fruit juices which are high in organic acids, have been explored as substitutes for inorganic acids to eliminate secondary acid waste and minimize toxic emission. [20-24]

Biohydrometallurgy promises a cost-effective and environmentally benign alternative to traditional metal extraction procedures from spent LIBs [25-28]. Bioleaching technology has been widely used for many years to extract valuable metals such as cobalt, nickel, manganese, and copper from ores and other secondary sources. Microorganisms such as bacteria (e.g., *Acidithiobacillus ferrooxidans*, *Acidithioacillus thiooxidans*, and *Leptospirillum ferrooxidans*)

and fungi (e.g., *Aspergillus* and *Penicillium* species) can mediate the bioleaching processes for the recovery of metals from metal-rich secondary resources such as ores, LIBs, and PCBs [29, 30] [31-34]. Acidophilic bacteria such as *A. ferrooxidans* generate acids like H_2SO_4, while; fungus *A.niger* produces organic acids that can solubilize metals from waste materials. The microbe-assisted bioleaching system involves the bio-oxidation process to dissolve insoluble metal components into water-soluble metals. The microorganism generates its energy by breaking ores or wastes into its metal components. Metal extraction by bioleaching process from LIBs used in coin cells, mobile phones, laptops, and secondary batteries has been reported using above mentioned microorganisms [35-38]. At low pulp densities (5 g/L - 40 g/L), these bioleaching processes were carried out for 10-15 days to achieve 80-95 % leaching efficiency. Among all viable options, *Acidithiobacillus ferrooxidans* appears to be a good candidate for bio-metal extraction in LIBs and other e-wastes due to their ease of growth, safe handling, and endurance at high acidic environments [39, 40, 41 42, 43]. The bioleaching of LIBs at high pulp density is still a challenging process due to microbial inhibition at high metal concentrations and substrate (iron) constraints at high viscosities. We had studied the bioleaching of $LiCoO_2$ and NMC-based LIBs with high leaching efficiency of valuable metals such as Co, Ni, Mn, and Li at a high pulp density of (100 g/L) using *Acidithiobacillus ferrooxidans* [44, 45]. However, the experiment duration was still 24 h per cycle. In order to optimize our process further, we continued using *Acidithiobacillus ferrooxidans* for bio-leaching experiments with the objective of reducing reaction time as well as regenerating the battery materials from the bioleaching process.

The recovery of metals to regenerate the cathode material is a critical step to close the loop of recycling. Due to the variable solubility of metals at different pHs, chemical precipitants such as sodium hydroxide (NaOH), sodium oxalate ($Na_2C_2O_4$), sodium carbonate (Na_2CO_3), sodium phosphate (Na_2HPO_4), and other ammonium counterparts are commonly

employed to separate metals from complex leach solutions [46-48]. Formal cathode regeneration approaches could be hydrothermal treatment, solid-state reaction (calcination), co-precipitation of metals, and sol-gel reaction after precipitating metals at a specific pH [49, 50]. In current LIBs technology, besides olivine-structure material ($LiFePO_4$), lithium metal oxides (e.g. $LiCoO_2$, $LiNiO_2$, $LiNi_xMn_yCo_zO_2$) have broad application as cathode materials, appraised as the most valuable battery component [48, 49, 51, 52]. The battery cathode materials market was valued at USD 15.27 billion in 2017 and is expected to grow at a CAGR (Compound Annual Growth Rate) of 6.2% to USD 22.17 billion by 2023 [6, 53]. The regeneration of cathode materials from bioleaching liquor is an innovative and environmental-friendly approach with substantial economic benefits in the reusability of valuable metals such as Ni, Mn, Co, and Li from spent LIBs. The profit from recycling a ton of spent LIBs via hydrometallurgy followed by regenerating electrode materials is approximately $10,440 [51, 54].

Most prior reports on the regeneration of LIB cathode materials used acid leachings such as H_2SO_4/H_2O_2, oxalic acid, phosphoric acid, and others, and the batteries were obtained from various sources such as coin cells, mobile phones, laptops, and electric cars [50, 52, 55-57]. While the regeneration of cathode materials from hydrometallurgical leachate has been widely reported, cathode recovery from bioleaching liquor containing a high amount of Fe has not yet been examined in most bioleaching reports. Unlike other studies where the experimental battery waste had minimal impurities and was homogenous due to manual sorting and pre-treatment step, we collected NMC-based LIBs from various sources with different manufacturers. Following the in-house developed sorting procedure, the batteries were then discharged, shredded together, and finely pulverized before use. The resulting black mass was more inhomogeneous that illustrating the resemblance of commercial battery recycling [58]. Our study aims to extract valuable metals from NMC-based LIBs at a high pulp density with high leaching efficiency in a shorter period by the bioleaching process using *Acidithiobacillus*

ferrooxidans and recovering the cathode material to close the loop of the technology. The metal concentration in the leached liquor was determined using ICP-OES. One limitation of the bio-leaching approach is the high amount of impurities, which pose a detrimental effect on the cathode regeneration process. We established a novel cleaning process combined with air oxidation and pH adjustment to effectively remove the high content of Fe from bacterial culture as well as Al and Cu, which are common impurities in leaching liquor. The extracted metals in the leaching liquor were then regenerated as NMC cathode materials via oxalate precipitation followed by high-temperature calcination. XRD and SEM-EDX were used to characterize the regenerated NMC cathode materials. Finally, the regenerated cathode materials are used to fabricate new batteries, followed by testing their electrochemical performances in a coin cell.

Experimental

Black mass preparation from spent NMC-based LIBs

The spent LIBs were collected from Nanyang Technological University in Singapore and classified according to cathode material types using an internally established XRF-based sorting technique before being mechanically processed. All sorted spent LIBs were first completely discharged with 20 % NaCl for 24 hours and then dried before being shredded by a mechanical shredder. The steel casings and plastic coverings were manually separated. The shredded battery materials were finely crushed and sieved through 100 m (160 mesh) using a table-top blender, then dried at 60 °C overnight [45].

Bacterial Growth and bioleaching experiments

DSMZ Germany supplied the native *A.ferrooxidans* strain (DSMZ 1927), which was isolated from mine water in Austria. The bacteria were grown on "Modified 9K" media [44, 45] containing $(NH_4)_2SO_4$ (0.5 g/L), KCl (0.05 g/L), K_2HPO_4* $3H_2O$ (0.2 g/L), $MgSO_4$* $7H_2O$ (0.5 g/L), $Ca(NO_3)_2$ (0.01 g/L), and $FeSO_4$* $7H_2O$ (135.0 g/L). To enhance the H_2SO_4 and ferric ions levels in the bacterial culture, the $FeSO_4$ dose was increased from 44.2 g/L to 135 g/L of

the original medium (3 fold). The pH of the "Modified 9K" media was adjusted to 2.0 with 2 M H_2SO_4 before sterilizing with a filtration device. In a 500 ml Erlenmeyer flask, 30 ml bacterial inoculum (10 % (v/v) (to promote bacterial growth in a short period) was added to 270 ml Modified 9K medium. Bacterial growth was induced by shaking at 170 rpm at 30 °C in an incubator. After 7 days of cultivation, the bacteria reached the logarithmic growth phase (ORP & Fe^{3+} concentration are constant); also, the concentration of H_2SO_4 reached 0.5 M. The Fe^{3+} formation and biogenic sulphuric acid production before the bioleaching process was estimated by the reported protocol using 5-sulfosalicylic acid (SSA) and acid-base titration method [44, 45].

Bioleaching experiments were carried out by adding 10 g NMC black mass in 100 ml bacterial culture (7 days culture) in 250 ml flasks (S/L 100 g/L) and shaking at 170 rpm at 30 °C. The bioleaching residue was separated from the leaching liquid every 2 h by filtration, and the system was replenished with a fresh bacterial culture. The bioleaching studies were performed again for the coming 2 h. Three cycles were completed all together. The leaching efficiency of the main elements nickel, manganese, cobalt, and lithium, as well as low abundance elements like iron, copper, and aluminium was determined for each cycle and added to achieve the overall recovery for 3 cycles. The metals' leaching efficiency following the bioleaching process was determined by comparing the aqua regia leaching values of NMC black mass.

$$\text{Metal leaching efficiency (\%)} = \frac{A}{B} \text{ X } 100 \qquad (1)$$

A = metal concentration in bioleaching, B = metal concentration in aqua regia leaching

Separation of Fe, Al, and Cu from the bioleaching solution

Common contaminants in the black mass of NMC-based LIBs include iron, aluminium, and copper from metal casing and electrode coating foils [48]. The presence of the contaminant has a detrimental impact on the quality of recovery material. The leaching liquor from the three

bioleaching cycles was accumulated, and 100 ml of the leaching liquor was used for progressive pH adjustment to 5.0. 5.5, 5.8, and 6.4 by 2N NaOH. In each step, the solution was stirred for 2 h and settled for 1 h to maximize air oxidation of ion Fe^{2+}. The precipitate was removed by centrifugation at 9000 rpm for 5 minutes. ICP-OES analyzed the supernatant to determine the primary metal contents and the presence of impurities.

Oxalate precipitation of Ni, Mn, and Co and synthesis of cathode material

50 ml of bioleachate (source) was neutralized to pH 6.0 prior to the metal recovery step, along with overnight air purging for air oxidation before the metal recovery step. Based on ICP-OES results, 50 ml of leaching supernatant was mixed with a sufficient amount of 0.3 M ammonium oxalate solution in a 250 ml round-bottom flask. The stirring speed was set at 1000 rpm for 1 h. Afterwards, the precipitate was collected by filtration using a PES membrane filter, 0.45 μm. The supernatant was collected for further Li-ion recovery. ICP-OES analysis was conducted to determine the content of Ni, Mn, and Co in obtained precipitate before synthesis. After precipitation, the metal ion ratio between Ni:Mn:Co in oxalate precipitation was adjusted to 1:1:1 or 6:2:2 by mixing with $MnNO_3 \cdot 6H_2O$ and $CoNO_3 \cdot 7H_2O$ in ethanol. The mixture was finally added with LiOH before calcination at 450 °C for 5 h. The product was ground to a fine powder after cooling to room temperature to ensure no agglomerates and sintered at 750 ℃ for 5 h and 900 ℃ and 850 ℃ for 10 h respectively for NMC 111 and NMC 622. The product phase was characterized by XRD (Bruker AXSD8 Advance), and the morphologies of the samples were determined using SEM-EDX analysis (Joel SU8010); the material composition was calculated from SEM-EDX.

Electrochemical Testing of regenerated NMC cathode materials

The electrochemical performance of NMC cathode powder was studied on Li-half coin cell configuration. To prepare electrode composite, NMC cathodic powder, conductive carbon

(acetylene black), and Polyvinylidene fluoride (PVDF) were dissolved in N-Methyl-2-pyrrolidone (NMP) by w/t 8:1:1 and uniformly mixed to get the slurry. The slurry was coated on aluminium foil and dried at 70 ℃ overnight before round punching with a 16mm diameter. The cut foil was dried in a vacuum oven for 8 h at 110 ℃ and transferred to the glovebox for assembly. Lithium metal was used as a counter electrode, while NMC or graphite acted as a working electrode. The electrolyte was EC:DEC (1:1). Galvanostatic charge-discharge was carried out between 2.5 and 4.5 V at ambient conditions using a Neware battery tester.

Analytical Instruments

The pH and redox potential were measured at 25 °C using pH and redox electrodes on a Mettler Toledo pH meter (Seven Compact S220). ICP-OES was used to determine the metal concentration in the leaching liquid and cathode materials (Perkin Elmer optima 8000). Scanning Electron Microscopy (SEM-EDX) (JSM-7600F Joel, Japan) was used to determine the surface morphology and composition of cathode materials, as well as the mapping of metals in native NMC black mass and bioleaching residues. The crystal structure of the cathodic material present in the LIBs before and after bioleaching was characterized by X-ray diffraction analysis using a Bruker powder diffractometer (AXS D8 advance) with Cu K radiation (WL=1.54060) and a voltage of 40 kV and 40 mA current.

Results and Discussion

NMC black mass characterization and bioleaching experiments

The phase composition and morphology of black mass were characterized by XRD and SEM analysis. Metal and element compositions were determined by ICP-OES and EDX. The results are indicated in Figure 1. ICP-OES analysis is more accurate as EDX analysis is semi-quantitative. Hence, quantification results from ICP-OES were used to report leaching efficiency and metal concentrations.

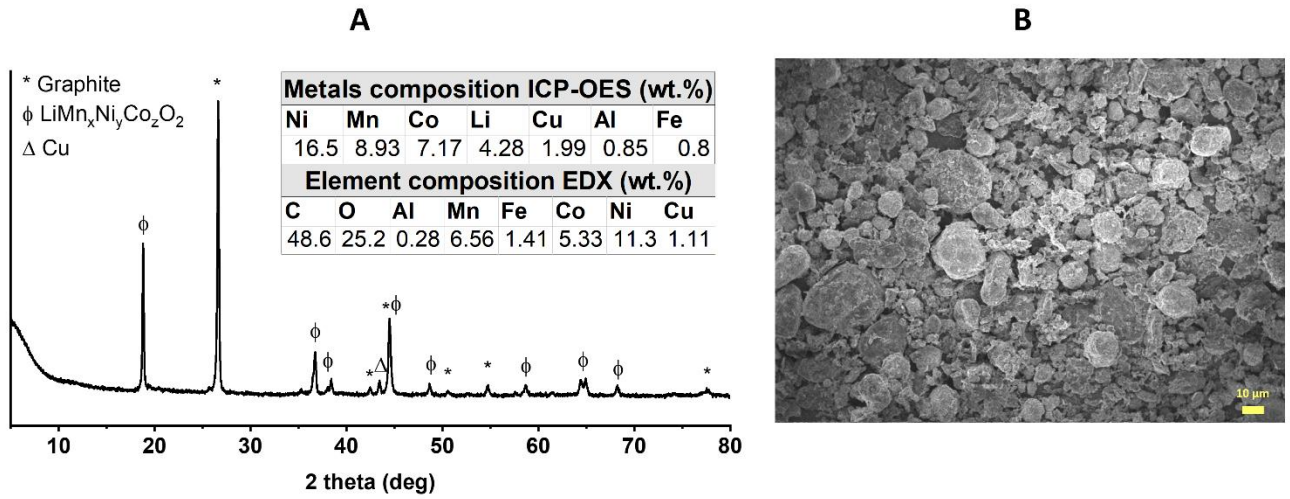

Figure 1. (A) XRD pattern of NMC black mass, (inset) metal composition calculated from ICP-OES and EDX ; (B) SEM of NMC black mass

The efficiency of *A. ferroxidan* in the bioleaching of NMC-based LIBs high pulp densities was reported in our previous report [44, 45]. In this study, bioleaching was performed using slightly modified media in a shorter time. 100 ml of the bacterial culture was placed into 250 ml Erlenmeyer flasks after 7 days of cultivation, which had entered the stationary phase (ORP & Fe^{3+} constant), and the biogenic H_2SO_4 concentration had reached 0.5 M. The flask was then loaded with 10 g of NMC black mass and kept in a shaking incubator at 30 °C at 160 rpm. After 2 h, the leaching liquor was collected and filtered from the residue. Again the bioleaching residue was replenished with 100 ml bacterial culture, and the experiments were continued for another 2 h, and a total of 3 cycles of bioleaching was performed. Previously, replenishing studies had been performed every 24 h, but after conducting the kinetic studies, it was found that 2 h is sufficient for each bioleaching cycle (data not shown).

Metals are dissolved during the bioleaching process by converting insoluble Ni^{3+}, Mn^{4+}, and Co^{3+} to soluble Ni^{2+}, Mn^{2+}, and Co^{+2} through a series of biological processes and subsequent acid dissolution [33, 59]. The reaction was initiated by the Fe^{3+} ion, which was further accompanied by the dissolution of insoluble metal ions by biogenic H_2SO_4. To break the battery

particles and discharge all metals from the interior region, a more significant concentration of H_2SO_4 and Fe^{3+} (bio-lixiviants) is required [44, 45]. This process used a considerable amount of biogenic H_2SO_4, which caused the pH to rise; however, the system's biogenic H_2SO_4 generation was sufficient, so the pH only slightly increased. Direct acid dissolution by biogenic H_2SO_4 released lithium from NMC powder. The sulfur metabolism of A. ferrooxidans, on the other hand, triggers the production of intermediate sulfates of Co, Ni, Mn, and Li, which aid the dissolution of metals in the leaching solution. The metal leaching mechanism reported by Xin et al. shows Fe^{2+}/Fe^{3+} redox reaction involving the acid dissolution of metals for the NMC-based LIB (Eqns 2-6) [33, 59].

$$4Fe^{2+} + O_2 + 4H^+ \longrightarrow 4Fe^{3+} + 2H_2O \quad (2)$$

$$Li_2O + 2H^+ \longrightarrow 2Li^+ + H_2O \quad (3)$$

$$M^{4+}/M^{3+}\ (M=Mn, Co, Ni) + Fe^{2+} \longrightarrow M^{2+}\ (MO) + Fe^{3+} \quad (4)$$

$$MO + 2H^+ \longrightarrow M^{2+} + H_2O \quad (5)$$

$$6LiNi_{1/3}Mn_{1/3}Co_{1/3}O_2 + 12H_2SO_4 + 6FeSO_4 \longrightarrow 3Fe_2(SO_4)_3 + 2MnSO_4 + 2NiSO_4 + 2CoSO_4 + 3Li_2SO_4 + 12H_2O \quad (6)$$

After three replenishing cycles with fresh bacterial culture, the leaching efficiency increased to 85.50% Ni, 91.83% Mn, 90.37 % Co, and 89.89 % Li in 6 h (Table 1). The best performing inorganic acid leaching of spent commercial LIBs with high leaching efficiency was reported at 200 g/L black mass using 1.75 M HCl at 50 °C for 2 h. The leaching efficiency was reported as 99.2% for Li, 99.0% for Mn and 98.0% for Co [60]. When the extraction was performed at the pulp density of 50 g/L with various organic acids such as citric acid, L-tartaric acid, oxalic acid, malic acid etc., a leaching efficiency of >90 % was achieved for the above metals [21]. Although the pulp density used in this bioleaching process (100 g/L) was higher than the organic acids reported for metal extraction, we could still achieve reasonably high efficiency between 85% to 97% of the above metals. As the bacterial culture has a significant amount of Fe^{3+} ions, the unused ferric ions go into the leaching solution and increase their

content compared to the other metal contents. The bioleaching process should really be cost-efficient with excellent metal recovery because the growth nutrient' cost (for bio-lixiviants production such as Fe^{3+} and H_2SO_4) production and other utilities are minimized when performing the process at high pulp densities.

Table 1. Leaching efficiency of metals after 3 cycles of 2h bioleaching process at a pulp density of 100g/L

Pulp density of LIB powder	Bacteria/ Media	Metals	1st cycle 2 h leaching %	2nd cycle 2 h leaching %	3rd cycle 2 h leaching %	Total 6 h Leaching %	Metal recovery g/Kg black mass
100g/L	*Acidithiobacillus ferrooxidans*	Ni	28.59±0.14	39.16±0.87	17.76±0.10	85.50	132.70
		Mn	30.79±0.47	42.20±0.24	18.84±0.22	91.83	80.81
		Co	27.24±0.21	36.47±0.41	26.66±0.32	90.37	62.42
		Li	33.74±0.43	38.86±0.08	17.29±0.20	89.89	33.44
		Cu	1.68±0.01	60.64±0.05	18.67±0.03	80.99	16.12
		Al	6.40±0.03	19.26±0.02	8.58±0.02	34.24	2.91
		Fe	>100	>100	>100	>100	276.02

Removal of Cu, Al, Fe from the bioleaching liquor

After 3 cycles of bioleaching experiments, the leaching liquor from all cycles was accumulated for further processing. Besides Cu^{2+} and Al^{3+}, the bioleaching liquor contains a significant amount of Fe, which can exist in Fe^{2+} and Fe^{3+} oxidation states. Hence, it is necessary to remove metal impurities before regenerating cathode materials. Conceptually, these metal ions could be selectively removed by pH adjusting, also known as hydroxide precipitation, which is a chemical precipitation technique in which metal hydroxides are formed when sodium hydroxide is used as the precipitating agent [46, 50]. According to literature, Fe^{3+} can selectively precipitate at pH 3; meanwhile, Cu^{2+} and Al^{3+} can remove as hydroxide precipitate at pH above 4 and 4.5, respectively [61]. The precipitation condition is also dependent on the concentration of metal ions; for example, Cu will precipitate as $Cu(OH)_2$ above pH 6.0

at extremely low concentrations. The reaction of Fe, Cu, and Al precipitation by NaOH is described below (Eqns 6-8).

$$CuSO_4 + 2NaOH \rightarrow Na_2SO_4 + Cu(OH)_2 \downarrow \quad (7)$$

$$Fe_2(SO_4)_3 + 6NaOH \rightarrow 3Na_2SO_4 + 2Fe(OH)_3 \downarrow \quad (8)$$

$$Al_2(SO_4)_3 + 6NaOH \rightarrow 3Na_2SO_4 + 2Al(OH)_3 \downarrow \quad (9)$$

Preliminary findings (Table S1) revealed that adjusting the pH of leachate to 4.8 could selectively remove Cu^{2+}, $Al^{3+,}$ and Fe^{3+} while minimizing the precipitation of Ni, Mn, and Co. The presence of Fe^{2+} ($FeSO_4.7H_2O$ nutrient unutilized by bacteria) remains a persistent problem for selective metal recovery. Fe^{2+} would only be removed at neutral conditions (pH 7 – 8). The proportion of oxidized Fe^{2+} over Fe^{3+} could vary from batch to batch, depending on the bacterial nutrient utilization. The fraction of Fe^{2+} in total Fe could be estimated by the proportion of Fe in the solution at pH 5 (without air oxidation) and total Fe in the solution initially (pH 2.5). At pH 4.5 – 5 without air oxidation (or immediate precipitation), Fe^{3+} will precipitate, and Fe^{2+} will be stable in the solution. The results suggest that it is possible to increase the pulp density further. Increases in leachate pH could cause coprecipitation of Ni^{2+} and Co^{2+}, which begin to precipitate at pHs greater than 5. To resolve the problem related to Fe^{2+}, Fe^{2+} ions must be completely oxidized to Fe^{3+} before precipitation (Eqn 9). One possibility is to expose leachate to air for oxidation. Long-time agitation was employed to maximize air dissolution in water and thus, facilitate Fe^{2+} oxidation.

$$Fe^{2+} + O_2 + 4H^+ \rightarrow Fe^{3+} + 2H_2O \quad (10)$$

To optimize the impurity cleaning condition, the pH of Fe-rich bio-leaching liquor was adjusted progressively from 2.5 to 5.0. 5.5, 5.8, and 6.4, along with 3 hours of agitation. Long-time agitation was employed to maximize air dissolution in water, facilitating Fe^{2+} oxidation to Fe^{3+} (Table 2). At pH 5.05, the amount of Cu^{2+} was reduced by half, at ~200 ppm, while only 20% of Al^{3+} was removed by precipitation. A substantial amount of Fe remained in the liquor

(~4300 ppm), then further pH adjustment is required. At pH 6.37, most of the Fe had been precipitated out of the supernatant. The amount of Fe, Cu, and Al remaining was accounted for less than 5% of all metal ions in the solution, suitable for the next recovery step. The decrease in the concentration of targeting elements (Li, Ni, Mn, Co) was obtained due to the dilution during pH adjustment and partially precipitation of metals hydroxide. According to a previous report, Ni^{2+}, $Co^{2+,}$ and Mn^{2+} tend to precipitate under conditions with a pH of 5.8 above. However, the solubility of [Ni^{2+}] and [Co^{2+}] is relatively higher than [Cu^{2+}] in neutral pH conditions. For example, at pH 6.5, the solubility of Cu^{2+} and Ni^{2+} is 3 mg/L and 32000 mg/L, respectively [50]. In brief, pH 6.0 adjustment along with Fe^{2+} air oxidation was chosen as the previous step before oxalate precipitation to regenerate cathode materials. Using O_2 to oxidize Fe^{2+} to Fe^{3+} might consume time, but it appears a cost-effective, effortless, and environmentally friendly solution to resolve the retaining Fe^{2+}. Alternatively, by the same concept, the rate of Fe^{2+} oxidation might be improved by using other oxidizing agents, such as $KMnO_4$, which requires careful control of elemental concentrations. We will explore this approach in the near future. Up to now, air oxidation still appears as a cost-effective and environmentally friendly method. In addition, the presence of Fe^{2+} could be utilized for further leaching reaction; hence, the pulp density could be increased further.

Table 2. Metal concentration (ppm) and percentage of metal retention in the bioleaching liquor after progressive pH adjustment

Metals	Source pH 2.5	1st PPtion pH 5.0		2nd PPtion pH 5.5		3rd PPtion pH 5.5		4th PPtion pH 5.8		5th PPtion pH 6.4	
	(ppm)	(ppm)	(%)	(ppm)	(%)	(ppm)	(%)	(ppm)	(%)	(ppm)	(%)
Ni	3977.8	3728.1	93.7	3420.6	86.0	3365.6	84.6	3312.6	83.3	3031.2	76.2
Mn	2249.8	2161.6	96.1	2121.2	94.3	2114.3	94.0	1961.3	87.2	1814.9	80.7
Co	1947.9	1824.2	93.7	1797.3	92.3	1761.3	90.4	1590.7	81.7	1490.0	76.5
Li	919.9	882.2	95.9	902.7	98.1	866.2	94.2	856.6	93.1	827.3	89.9
Cu	461.3	215.5	46.7	147.0	31.9	138.1	29.9	105.6	22.9	43.0	9.3
Al	105.1	84.9	80.8	76.7	73.0	68.0	64.7	66.8	63.5	48.0	45.7
Fe	7475.5	4360.8	58.3	2758.9	36.9	1821.4	24.4	591.7	7.9	120.5	1.6

Oxalate precipitation

The accumulated bioleachate source was neutralized to pH 6.0 before the metal recovery step, along with air purging for air oxidation. The Co/Mn/Ni concentration was slightly reduced due to precipitation and dilution, as shown in table 3. Meanwhile, the leachate was completely depleted of Cu and Fe. There was still 1.6 % Al left in the liquor. However, the amount of Al is negligible when compared to the amounts of Li, Ni, Mn, and Co ions, which might not affect the purity of precipitation. In fact, the presence of trace amounts of Al as dopant could stabilize the lattice structure, then enhance the capacity retention as well as rate performance of cathode material [62, 63]. Currently, oxalate and carbonate are the reagents commonly used to precipitate Ni, Co and Mn in LIBs recycling studies. Oxalate precipitation for Mn, Co and Ni occur at a wide range of pH conditions. In contrast, the solution needs to be adjusted to alkaline (pH > 9). when using carbonate as the precipitating reagent. Therefore, oxalate was chosen in this study not to complicate the process by including another pH adjustment step.

Table 3. Metal concentration (ppm) of accumulated NMC leaching solution (source), solution after air purging and pH precipitation, and supernatant after oxalate precipitation, the last column is the % of metal ion obtained from precipitation based on ICP-OES calculation. The total amount of precipitation is 2488 mg.

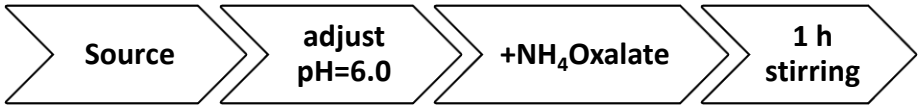

Metal	Source	Air purging pH=6.0		Supernatant	Precipitate *
	(ppm)	(ppm)	(%)	(ppm)	(wt %)
Li	1899.0	1960.0	~100.0	1091.0	0.33
Co	3169.0	2707.4	85.4	N.D	5.94
Mn	4288.0	3961.9	92.4	73.1	8.06
Ni	7712.0	5932.7	76.9	88.3	12.27
Cu	1046.0	N.D	Nil	N.D	0.22
Fe	1174.0	N.D	Nil	N.D	N.D
Al	3010.0	48.2	1.6	N.D	0.13

* The remaining wt % of precipitate are non-metallic elements (e.g., C, O, H)

The leaching supernatant was mixed with a 0.3 M ammonium oxalate $(NH_4)_2C_2O_4$ solution and vigorously stirred at 1000 rpm for 1 hour for recovery purposes. The oxalate ion was chosen as a precipitating agent because of its capacity to coordinate with metal ions, such as Ni^{2+}, Co^{2+}, or Mn^{2+}, to form a five-membered ring structure oxalate complex. These compounds frequently precipitate as solids due to their limited solubility, whereas lithium usually dissolves in oxalic solution. The oxalate product was characterized by ICP-OES after the precipitation and drying to determine the metal composition. The calculated amount of metal ions in the precipitate (in mg) is illustrated in Table 3. Co^{2+}, Mn^{2+}, and Ni^{2+} ions were

successfully recovered as oxalate-precipitate from leaching liquor, as can be observed. The trivial trace amount of Cu and Al in the product could act as doping elements and enhance electrochemical cycling behaviour. The supernatant has a negligible amount of Mn and Ni, indicating the proposed process's high selectivity and efficacy. In addition, the supernatant now contains solely Li-ions, which can be recovered directly as Li_2CO_3 or Li_3PO_4 at pH above 11 [64]. The recovery of Li-ion has been extensively developed and reported; therefore, it was not be covered in this study.

The presence of oxalate in wastewater might require additional treatment steps before releasing to the environment. The risk could be reduced significantly by either controlling the amount of oxalate in the precipitation process or reusing the wastewater as the oxalate source for subsequent batches of precipitation. In addition, based on the precipitation tendency of oxalate ions, there is a prospect of utilizing concentrated-oxalate wastewater from other industrial sources in the LIB recycling process.

Cathode material regeneration

NMC_{111} and NMC_{622} are the two most common types of NMC composition widely reported. NMC_{111} material typically offers good cycling stability, and NMC_{622} is known as high-voltage cathode material. Hence, we chose to synthesise NMC_{111} and NMC_{622} material from oxalate precipitate. Since Ni:Mn:Co ratio in the precipitate was not optimal to our desired ratio, the metal ratio needed to adjust before the annealing process. The corresponding nitrate salts were chosen to mix with the oxalate compound before the heat-treatment step to maintain the valence state of Ni, Mn, and Co ions. The sintering temperature of NMC_{111} was 900 °C, while the optimal temperature of NMC_{622} was 850 °C. The regenerated material was characterized using XRD, ICP-OES, SEM, and EDX after being obtained as the final product. ICP-OES and EDX analytical results showed that the chemical composition of regenerated

NMC cathodes is well aligned with the expected formula $LiNi_{0.3}Mn_{0.3}Co_{0.3}O_2$ and $LiNi_{0.6}Mn_{0.2}Co_{0.2}O_2$ (Table 4).

Table 4. The elemental molar ratio of regenerated NMC_{111} and NMC_{622} analysed from ICP-OES and EDX

Elements		Li	Ni	Mn	Co	Al	O
NMC_{111}-900 °C	**EDX**	NA	0.333	0.289	0.302	0.016	2.013
	ICP	1.058	0.338	0.345	0.366	0.00222	NA
NMC_{622}-850 °C	**EDX**	NA	0.578	0.211	0.201	0.008	2.228
	ICP	0.996	0.647	0.239	0.225	0.00255	NA

Figure 2 shows the XRD patterns of regenerated NMC_{111} and NMC_{622} cathode material in the 10–80° range. The regenerated NMC materials have layered structure and pure phase, which is well indexed to the reference PDF#00-062-0431, a library of LiNi0.3Mn0.3Co0.3O2 and conformity to commercial NMC. Two dominating peaks are corresponding to the (003) and (104) planes, as well as significant splitting of the (006)/(102) and (108)/(110) peaks implying a well-ordered hexagonal structure [57, 65].

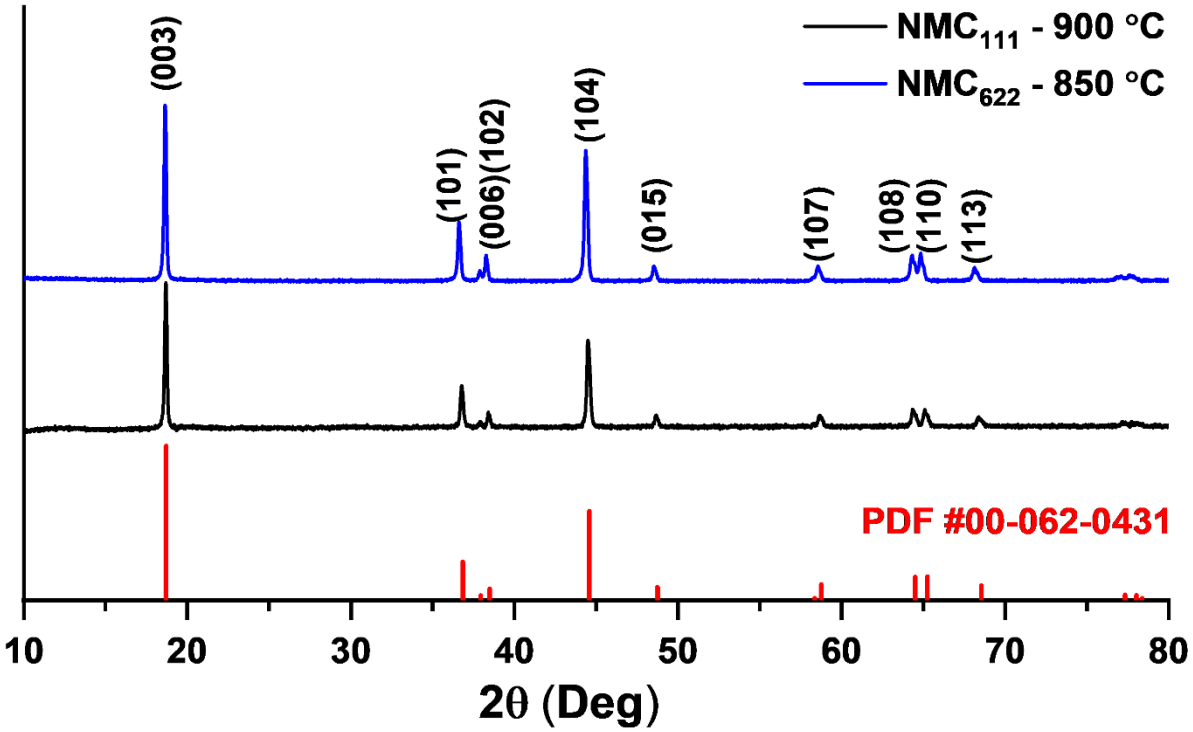

Figure 2. XRD pattern of regenerated NMC_{111}, NMC_{622} compared with the database of $LiNi_{0.3}Mn_{0.3}Co_{0.3}O_2$ (PDF #00-062-0431)

In relative to NMC_{111}, NMC_{622} had a lattice contraction along the c-axis and a lattice expansion along the a-axis based on the refinement parameter. XRD revealed a lattice parameter ratio (c/a) greater than 4.9, indicating good layer characteristics. The I(003)/I(104) ratios (intensity ratios of (003) and (104) peaks) were 1.4086 and 1.255, respectively, meeting the empirical criteria for low cation mixing (Table 5). Notably, while NMC_{111} was sintered at 900 ℃, however, the sintering temperature of NMC_{622} was only 850 ℃. At higher temperatures, the resulting NMC_{622} has a lower I(003)/I(104) ratio at 1.102, indicating a high degree of cation mixing (Figure S4). The phenomenon is described by partial disordering caused by Ni^{2+} migration from the transition-metal layer to the lithium layer caused by similar ionic radii of Li-ion (0.76Å) and Ni ion (0.69Å). [56, 65]. The sintering temperature optimization was explicitly reported by Yao et al. for NMC-based LIBs [66].

Table 5. Refined lattice parameter, lattice parameter ratio, and peak intensity ratio of (003) and (104)

Cathode Material	a (Å)	c (Å)	c/a	I(003)/I(104)
NMC_{111} -900 ^{o}C	2.864	14.244	4.972	1.408
NMC_{622} -850 ^{o}C	2.873	14.234	4.953	1.225

The morphologies of NMC_{111} and NMC_{622} cathode materials was investigated from SEM images (Figure 3). Generally, high magnification images of regenerated NMC materials showed primary particles with faceted surfaces in the size range of ~500 nm to ~ 1 μm similar particle shapes, relative to commercial NMC (ENAX) (Figure S3). There was an agglomeration of primary particles; however, unlike commercial material, the shape of the secondary cluster is ambiguous. Particle sizes of NMC_{622} were slightly larger than NMC_{111}. While a smoother morphology surface was observed for NMC_{111}, defections and uneven shapes were inevitably formed after calcination in NMC_{622}. It was explained by lower sintering temperature, which slows the grain growth of solid-state reaction [57]. Several shattered particles were attached to their surfaces, attributed to inhomogeneous reaction. In EDX mapping, a homogenous distribution of Co, Mn, and Ni was observed in both NMC_{111} and NMC_{622} cathode material (Figure S5 & S6).

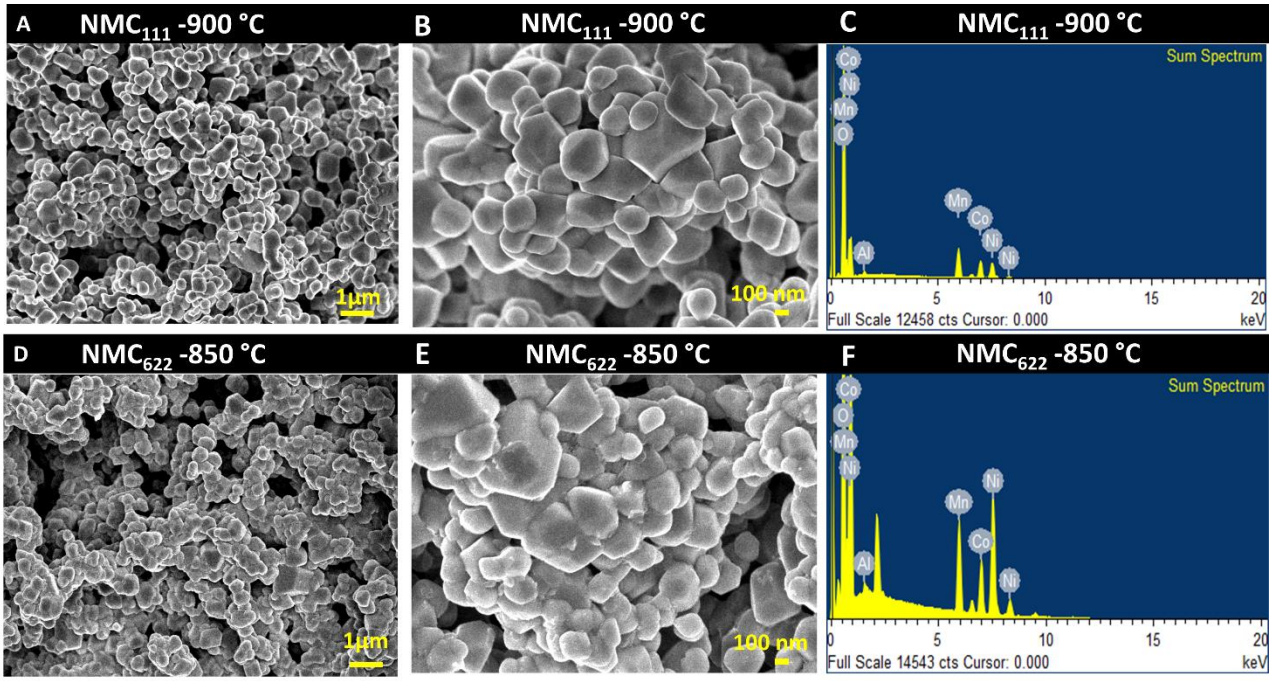

Figure 3. SEM images of NMC_{111} (sintering at 900 °C) (A, B), NMC_{622} (sintering at 850 °C) (D, E); EDX pattern NMC_{111}-900 °C (C), NMC_{622} -850 °C (F)

Electrochemical performance of regenerated cathode material

We tested the electrochemical performance of the regenerated materials in half coin-cell configuration using commercial NMC as a reference after successfully regenerating NMC cathode materials from the bioleaching process with expected composition, phase, and morphology. The counter and reference electrodes were made of lithium. As shown from Figure 4, where batteries were tested at 100 mA g^{-1}, regenerated NMC materials resembled commercial material's long-term cycling performance. In the first 25 cycles, commercial NMC had a slightly higher specific capacity than NMC_{111} and NMC_{622}. In particular, the initial discharge capacity of NMC_{111} and NMC_{622} were 112 and 109 mAh g^{-1}, respectively, while commercial NMC was 118 mAh g^{-1}. The capacity retention of regenerated NMC_{111}, NMC_{622}, and commercial NMC, after 50 cycles, were 89%, 84%, and 85% of the initial capacity. However, after 75 cycles, the discharge capacity of investigated material decreased to a similar

value in the range from 88 to 93 mAh g^{-1}. The good cyclability of NMC_{111} could be explained by a low level of cation mixing, as evidenced by XRD

Furthermore, compared to commercial NMC and other reported methods, the rate capability of NMC_{111} and NMC_{622} samples are within the acceptable range, which might be explained by showing similar morphology with commercial NMC material (Figure S3). NMC_{111} and NMC_{622} had a discharge capacity of 73 mAh g^{-1} at a high current rate of 400 mA g^{-1}, while the commercial NMC had a value of 69 mAh g^{-1}. The discharge capacity of NMC_{622} was more significant than the others after reverting to a low current rate of 50 mA g-1, which might be explained by the cracking defects on the morphological surface, which facilitated Li conversion.

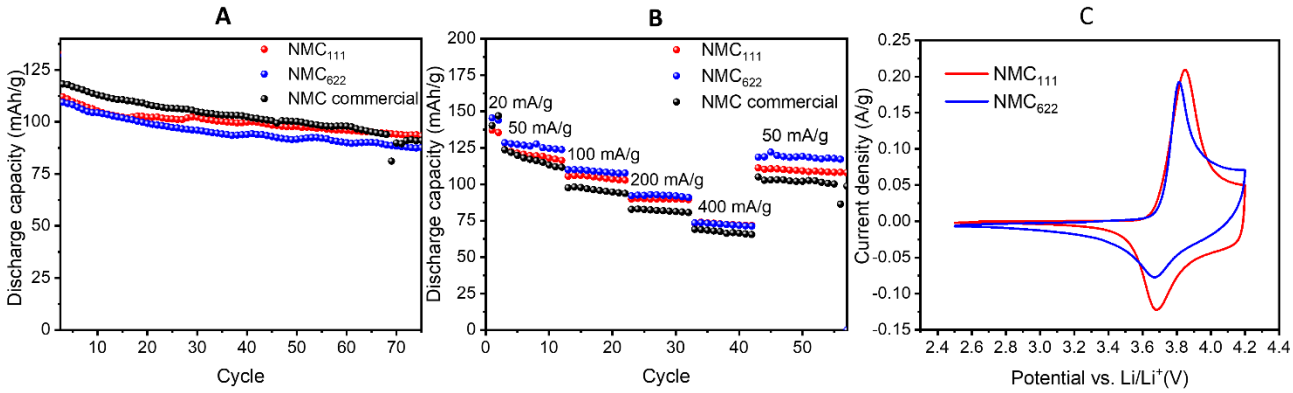

Figure 4. (A) Specific discharge capacity vs cycle of recycled NMC_{111}, NMC_{622}, and NMC commercial at the current density of 100 mA g^{-1}, (B) Specific discharge capacity of recycled NMC_{111}, NMC_{622}, and NMC commercial at various current rates of 20, 50, 100, 200 and 400 mA g^{-1} (C) Cyclic voltammetry of regenerated NMC_{111}, NMC_{622} in the potential range from 2.5 V to 4.2 V vs Li/Li^+, the sweeping rate at 0.1 mV/s

Further electrochemical studies were carried out for NMC_{111} and NMC_{622} half-cell, and the batteries were subjected to cyclic voltammetry study at a constant potential sweep of 0.1 mV/s in the voltage range from 2.5 V to 4.2 V vs Li/Li^+. The Cyclic voltammetric curves of NMC_{111} and NMC_{622} are quite similar, shown in Figure 4C. NMC_{111} has redox potential peaks

of 3.85 V and 3.68 V, slightly higher than NMC_{622}, with peaks of 3.81 V and 3.67 V, respectively. The current density of NMC_{111}, on the other hand, declined considerably after reaching its maximum during the charging process. In the meantime, NMC_{622} has shown only a gradual drop. At voltages greater than 4.0 V, the current density of NMC_{622} was greater than NMC_{111}. According to the findings, if the voltage window was increased to 4.5 V, regenerated NMC_{622} would have a better capacity than its regenerated NMC_{111} counterpart (Figure S7 & S8).

It was observed that the regenerated NMC_{111} and NMC_{622} materials seem to have inferior cycling performance compared with the commercial products. As the black mass derived from the source of mixed battery waste, the mass ratio between Mn, Ni and Co in the leachate and the co-precipitate differed from 1:1:1 and 6:2:2, respectively. Hence, $MnNO_3$ and $CoNO_3$ were added to the precipitate to adjust the element ratio. This might have resulted in compositional and functional heterogeneity of the product; in addition, the concentration of valuable metal ions (Mn, Ni and Co) in the lixiviant was practically high, which might affect the coprecipitation quality. To overcome the issue, further studies on optimization of the precipitation process and adjustment of elemental ratio should be conducted so that the formation rate and morphology of the product will be controllable. The flow chart of the whole recycling process is given in Figure 5.

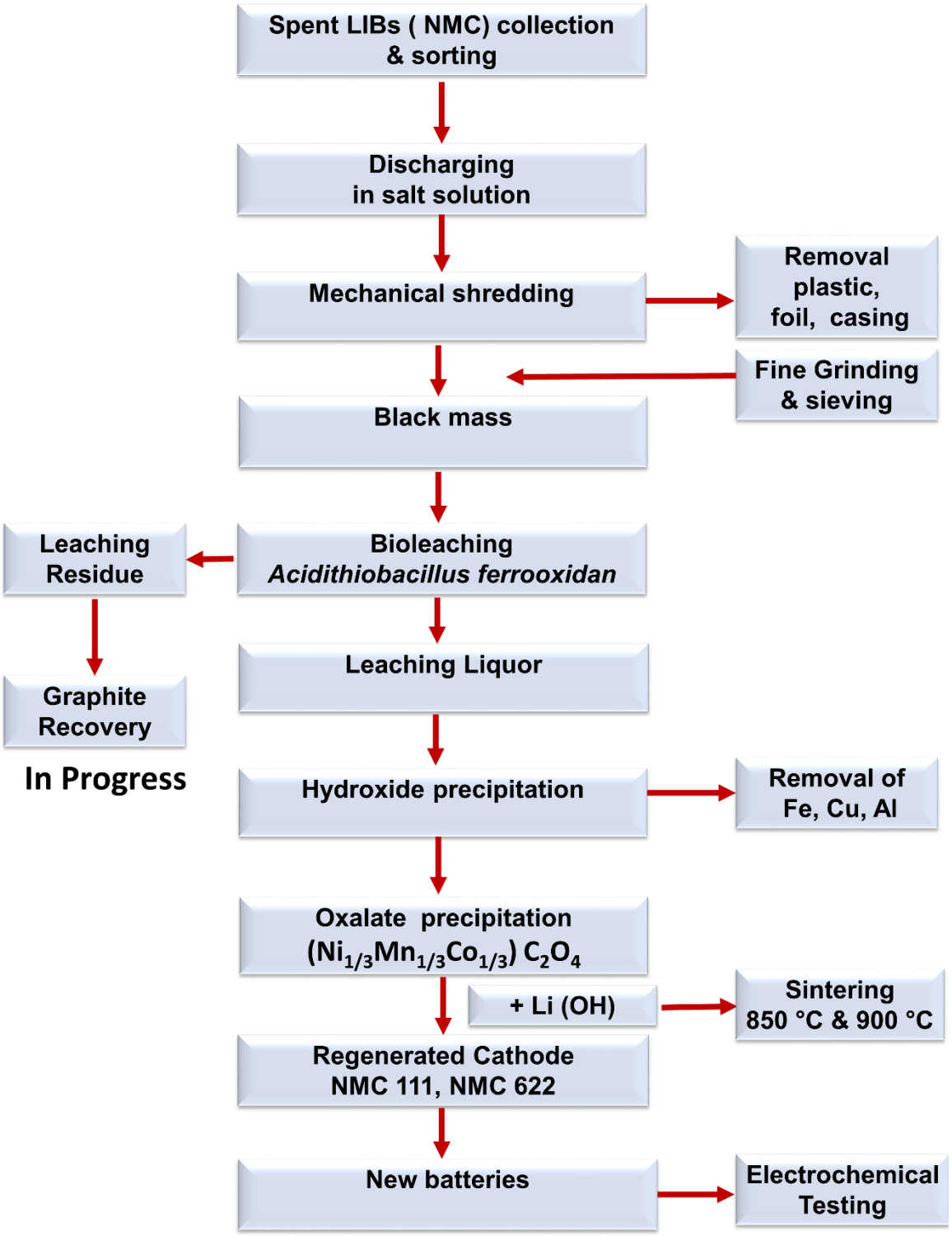

Figure 5. The whole process of cathode regeneration from NMC-based spent LIBs via the Bioleaching process

Conclusions

Our study has successfully demonstrated a closed-loop recycling process from end-of-life LIBs to cathode material regeneration using bioleaching approach. At a pulp density of 100g/L, Acidithiobacillus ferrooxidans-mediated bioleaching yielded 85.50 % Ni, 91.83 % Mn, 90.37 % Co, and 89.89 % Li in 3 cycles of the process for a total of 6 h, the least amount of time compared to other reports. By a comprehensive study on impurity removal conditions, we proved that the combination pH adjustment (pH of 6) and air-purging is efficient to remove significantly high content of Fe (from bacteria nutrient) and Al, Cu (from black mass). After obtaining impurity-free leachate, NMC_{111} and NMC_{622} were synthesized via oxalic co-precipitation and a series of heating treatment processes. The regenerated NMC_{111} and NMC_{622} cathode materials had a well-ordered structure and a low amount of cation mixing, and comparable electrochemical properties with commercial NMC cathode. NMC_{111} and NMC_{622} had initial discharge capacities of 112 and 109 mAh g^{-1}, respectively, whereas commercial NMC had an initial discharge capacity of 118 mAh g^{-1}. After 50 cycles at 100 mAh, the retention capacity of the regenerated NMC_{111} and NMC_{622} and commercial NMC was up to 89%, 84%, and 85%, respectively.

Supporting Information

Table S1. The metal concentration of leachate after progressive precipitation without aeration

Figure S1. XRD refinement of NMC_{111} (900 ℃)

Figure S2. XRD refinement of NMC_{622} (850 ℃)

Figure S3. (A and B) SEM images, and (C) EDX of commercial NMC (ENAX)

Figure S4. (A) XRD pattern (B) SEM images (C) Refined lattice parameter, lattice parameter ratio, and peak intensity ratio of (003) and (104) of NMC_{622} annealing at 900 ℃

Figure S5 (A) EDX mapping of recycled NMC_{111}, (B) elemental composition from EDX spectra

Figure S6 (A) EDX mapping of recycled NMC_{622}, (B) Elemental composition from EDX spectra

Figure S7. (A-E) Galvanostatic charge-discharge curves comparison between recycled NMC_{111}, NMC_{622}, and NMC commercial at 20 mA g^{-1} (A), 50 mA g^{-1} (B), 100 mA g^{-1} (C), 200 mA g^{-1} (D) and 400 mA g^{-1} (E) in the voltage range from 2.5 to 4.2 V vs Li/Li^+

Figure S8. Galvanostatic charge-discharge curves of recycled NMC_{111} (A, D), NMC_{622} (B, E), and NMC commercial (C, F); half cell at different current rates (A, B, C) and in different cycle numbers (D, E, F) in the voltage range from 2.5 to 4.2 V vs Li/Li^+

Acknowledgment

This research/project is supported by the National Research Foundation, Singapore, and National Environment Agency, Singapore, under its Closing the Waste Loop Funding Initiative (Award No. USS-IF-2018-4).

Disclaimer

"Any opinions, findings and conclusions or recommendations expressed in this material are those of the author(s) and do not reflect the views of National Research Foundation, Singapore, and the National Environment Agency, Singapore. "

Credit Author Statement

Minh Phuong Do and Joseph Jegan Roy has equally contributed to this work

Minh Phuong Do – Conceptualization, Methodology, Investigation, Validation, Writing - Original Draft, Writing - Review & Editing, Visualization

Joseph Jegan Roy – Conceptualization, Methodology, Investigation, Validation, Writing - Original Draft, Writing - Review & Editing, Visualization

Bin Cao- Conceptualization, Funding acquisition, Supervision, Writing - Review & Editing

Madhavi Srinivasan – Conceptualization, Funding acquisition, Project administration, Supervision, Writing - Review & Editing,

References

1. Zheng, X.; Zhu, Z.; Lin, X.; Zhang, Y.; He, Y.; Cao, H.; Sun, Z., A Mini-Review on Metal Recycling from Spent Lithium Ion Batteries. *Engineering* **2018,** *4* (3), 361-370, DOI 10.1016/j.eng.2018.05.018.

2. Chen, M.; Ma, X.; Chen, B.; Arsenault, R.; Karlson, P.; Simon, N.; Wang, Y., Recycling End-of-Life Electric Vehicle Lithium-Ion Batteries. *Joule* **2019,** *3* (11), 2622-2646, DOI 10.1016/j.joule.2019.09.014.

3. Zhao, S.; He, W.; Li, G., Recycling Technology and Principle of Spent Lithium-Ion Battery. In Recycling of Spent Lithium-Ion Batteries: Processing Methods and Environmental Impacts, An, L., Ed. Springer International Publishing: Cham, 2019; pp 1-26, DOI 10.1007/978-3-030-31834-5_1.

4. Xiao, J.; Li, J.; Xu, Z., Challenges to Future Development of Spent Lithium Ion Batteries Recovery from Environmental and Technological Perspectives. *Environ Sci Technol* **2020**, 54, 9-25, DOI 10.1021/acs.est.9b03725.

5. Luidold, S., Chapter 16 - Recycling of Technologic Metals: Fundamentals and Technologies. In *Sustainable Resource Recovery and Zero Waste Approaches*, Taherzadeh, M. J.; Bolton, K.; Wong, J.; Pandey, A., Eds. Elsevier: 2019; pp 223-238, DOI 10.1016/B978-0-444-64200-4.00016-5.

6. Mayyas, A.; Steward, D.; Mann, M., The case for recycling: Overview and challenges in the material supply chain for automotive li-ion batteries. *Sustainable Materials and Technologies* **2019,** *19*, e00087, DOI 10.1016/j.susmat.2018.e00087.

7. Wang, Y.; An, N.; Wen, L.; Wang, L.; Jiang, X.; Hou, F.; Yin, Y.; Liang, J., Recent progress on the recycling technology of Li-ion batteries. *Journal of Energy Chemistry* **2021**, 55, 391-419, DOI 10.1016/j.jechem.2020.05.008.

8. Xu, J.; Thomas, H. R.; Francis, R. W.; Lum, K. R.; Wang, J.; Liang, B., A review of processes and technologies for the recycling of lithium-ion secondary batteries. *Journal of Power Sources* **2008,** *177* (2), 512-527, DOI 10.1016/j.jpowsour.2007.11.074.

9. Li, G.; An, L., Impacts of Recycling of Spent Lithium-Ion Batteries on Environmental Burdens. In *Recycling of Spent Lithium-Ion Batteries: Processing Methods and Environmental Impacts*, An, L., Ed. Springer International Publishing: Cham, 2019; pp 199-217, DOI 10.1007/978-3-030-31834-5_8.

10. Ekberg, C.; Petranikova, M., Chapter 7 - Lithium Batteries Recycling. In *Lithium Process Chemistry*, Chagnes, A.; Światowska, J., Eds. Elsevier: Amsterdam, 2015; pp 233-267, DOI 10.1016/B978-0-12-801417-2.00007-4.

11. Ashiq, A.; Kulkarni, J.; Vithanage, M., Hydrometallurgical Recovery of Metals From E-waste. In *Electronic Waste Management and Treatment Technology*, 2019; pp 225-246, DOI 10.1016/b978-0-12-816190-6.00010-8.

12. Sun, L.; Qiu, K., Vacuum pyrolysis and hydrometallurgical process for the recovery of valuable metals from spent lithium-ion batteries. *Journal of Hazardous Materials* **2011,** *194*, 378-384, DOI 10.1016/j.jhazmat.2011.07.114.

13. Yin, H.; Xing, P., Pyrometallurgical Routes for the Recycling of Spent Lithium-Ion Batteries. In *Recycling of Spent Lithium-Ion Batteries: Processing Methods and Environmental Impacts*, An, L., Ed. Springer International Publishing: Cham, 2019; pp 57-83, DOI 10.1007/978-3-030-31834-5_3.

14. Xiao, J.; Li, J.; Xu, Z., Challenges to Future Development of Spent Lithium Ion Batteries Recovery from Environmental and Technological Perspectives. *Environmental Science & Technology* **2020,** *54* (1), 9-25, DOI 10.1021/acs.est.9b03725.

15. Sun, Z.; Cao, H.; Xiao, Y.; Sietsma, J.; Jin, W.; Agterhuis, H.; Yang, Y., Toward Sustainability for Recovery of Critical Metals from Electronic Waste: The Hydrochemistry

Processes. *ACS Sustainable Chemistry & Engineering* **2016,** *5* (1), 21-40, DOI 10.1021/acssuschemeng.6b00841.

16. Jiang, Y.; Chen, X.; Yan, S.; Li, S.; Zhou, T., Pursuing green and efficient process towards recycling of different metals from spent lithium-ion batteries through Ferro-chemistry. *Chemical Engineering Journal* **2021,** *426*, 131637, DOI 10.1016/j.cej.2021.131637.

17. Chen, X.; Kang, D.; Li, J.; Zhou, T.; Ma, H., Gradient and facile extraction of valuable metals from spent lithium ion batteries for new cathode materials re-fabrication. *Journal of Hazardous Materials* **2020,** *389*, 121887, DOI 10.1016/j.jhazmat.2019.121887.

18. Xuan, W.; de Souza Braga, A.; Korbel, C.; Chagnes, A., New insights in the leaching kinetics of cathodic materials in acidic chloride media for lithium-ion battery recycling. *Hydrometallurgy* **2021,** *204*, 105705, DOI 10.1016/j.hydromet.2021.105705.

19. Chabhadiya, K.; Srivastava, R. R.; Pathak, P., Two-step leaching process and kinetics for an eco-friendly recycling of critical metals from spent Li-ion batteries. *Journal of Environmental Chemical Engineering* **2021,** *9* (3), 105232, DOI 10.1016/j.jece.2021.105232.

20. Chen, X.; Luo, C.; Zhang, J.; Kong, J.; Zhou, T., Sustainable Recovery of Metals from Spent Lithium-Ion Batteries: A Green Process. *ACS Sustainable Chemistry & Engineering* **2015,** *3* (12), 3104-3113, DOI 10.1021/acssuschemeng.5b01000.

21. Meshram, P.; Mishra, A.; Abhilash; Sahu, R., Environmental impact of spent lithium ion batteries and green recycling perspectives by organic acids – A review. *Chemosphere* **2020,** *242*, 125291, DOI 10.1016/j.chemosphere.2019.125291.

22. Nayaka, G. P.; Pai, K. V.; Manjanna, J.; Keny, S. J., Use of mild organic acid reagents to recover the Co and Li from spent Li-ion batteries. *Waste Management* **2016,** *51*, 234-238, DOI 10.1016/j.wasman.2015.12.008.

23. Kumar, J.; Shen, X.; Li, B.; Liu, H.; Zhao, J., Selective recovery of Li and FePO4 from spent LiFePO4 cathode scraps by organic acids and the properties of the regenerated LiFePO4. *Waste Management* **2020,** *113*, 32-40, DOI 10.1016/j.wasman.2020.05.046.

24. Wu, Z.; Soh, T.; Chan, J. J.; Meng, S.; Meyer, D.; Srinivasan, M.; Tay, C. Y., Repurposing of Fruit Peel Waste as a Green Reductant for Recycling of Spent Lithium-Ion Batteries. *Environmental Science & Technology* **2020,** *54* (15), 9681-9692, DOI 10.1021/acs.est.0c02873.

25. Pollmann, K.; Kutschke, S.; Matys, S.; Raff, J.; Hlawacek, G.; Lederer, F. L., Bio-recycling of metals: Recycling of technical products using biological applications. *Biotechnol Adv* **2018,** *36* (4), 1048-1062, DOI 10.1016/j.biotechadv.2018.03.006.

26. Watling, H., Review of Biohydrometallurgical Metals Extraction from Polymetallic Mineral Resources. *Minerals* **2014,** *5* (1), 1-60, DOI 10.3390/min5010001.

27. Krebs, W.; Brombacher, C.; Bosshard, P. P.; Bachofen, R.; Brandl, H., Microbial recovery of metals from solids. *FEMS Microbiology Reviews* **1997,** *20* (3), 605-617, DOI 10.1016/S0168-6445(97)00037-5.

28. Mishra, D.; Kim, D.-J.; Ahn, J.-G.; Rhee, Y.-H., Bioleaching: A microbial process of metal recovery; A review. *Metals and Materials International* **2005,** *11* (3), 249-256, DOI 10.1007/BF03027450.

29. Schippers, A.; Hedrich, S.; Vasters, J.; Drobe, M.; Sand, W.; Willscher, S., Biomining: metal recovery from ores with microorganisms. *Adv Biochem Eng Biotechnol* **2014,** *141*, 1-47, DOI 10.1007/10_2013_216.

30. Kaksonen, A. H.; Boxall, N. J.; Gumulya, Y.; Khaleque, H. N.; Morris, C.; Bohu, T.; Cheng, K. Y.; Usher, K. M.; Lakaniemi, A.-M., Recent progress in biohydrometallurgy and microbial characterisation. *Hydrometallurgy* **2018,** *180*, 7-25, DOI 10.1016/j.hydromet.2018.06.018.

31. Baniasadi, M.; Vakilchap, F.; Bahaloo-Horeh, N.; Mousavi, S. M.; Farnaud, S., Advances in bioleaching as a sustainable method for metal recovery from e-waste: A review. *Journal of Industrial and Engineering Chemistry* **2019,** *76*, 75-90, DOI 10.1016/j.jiec.2019.03.047.

32. Bahaloo-Horeh, N.; Vakilchap, F.; Mousavi, S. M., Bio-hydrometallurgical Methods For Recycling Spent Lithium-Ion Batteries. In *Recycling of Spent Lithium-Ion Batteries: Processing Methods and Environmental Impacts*, An, L., Ed. Springer International Publishing: Cham, 2019; pp 161-197, DOI 10.1007/978-3-030-31834-5_7.

33. Roy, J. J.; Cao, B.; Madhavi, S., A review on the recycling of spent lithium-ion batteries (LIBs) by the bioleaching approach. *Chemosphere* **2021,** *282*, 130944, DOI 10.1016/j.chemosphere.2021.130944.

34. Bosecker, K., Bioleaching: metal solubilization by microorganisms. *FEMS Microbiology Reviews* **1997,** *20* (3), 591-604, DOI 10.1016/S0168-6445(97)00036-3.

35. Naseri, T.; Bahaloo-Horeh, N.; Mousavi, S. M., Bacterial leaching as a green approach for typical metals recovery from end-of-life coin cells batteries. *Journal of Cleaner Production* **2019,** *220*, 483-492, DOI 10.1016/j.jclepro.2019.02.177.

36. Diaz-Martinez, M. E.; Argumedo-Delira, R.; Sanchez-Viveros, G.; Alarcon, A.; Mendoza-Lopez, M. R., Microbial Bioleaching of Ag, Au and Cu from Printed Circuit Boards of Mobile Phones. *Curr Microbiol* **2019,** *76* (5), 536-544, DOI 10.1007/s00284-019-01646-3.

37. Gu, F.; Summers, P. A.; Hall, P., Recovering materials from waste mobile phones: Recent technological developments. *Journal of Cleaner Production* **2019,** *237*, 117657, DOI 10.1016/j.jclepro.2019.117657.

38. Heydarian, A.; Mousavi, S. M.; Vakilchap, F.; Baniasadi, M., Application of a mixed culture of adapted acidophilic bacteria in two-step bioleaching of spent lithium-ion laptop batteries. *Journal of Power Sources* **2018,** *378*, 19-30, DOI 10.1016/j.jpowsour.2017.12.009.

39. Biswal, B. K.; Jadhav, U. U.; Madhaiyan, M.; Ji, L.; Yang, E.-H.; Cao, B., Biological Leaching and Chemical Precipitation Methods for Recovery of Co and Li from Spent Lithium-Ion Batteries. *ACS Sustainable Chemistry & Engineering* **2018,** *6* (9), 12343-12352, DOI 10.1021/acssuschemeng.8b02810.

40. Quatrini, R.; Johnson, D. B., Acidithiobacillus ferrooxidans. *Trends Microbiol* **2019,** *27* (3), 282-283, DOI 10.1016/j.tim.2018.11.009.

41. Zhang, S.; Yan, L.; Xing, W.; Chen, P.; Zhang, Y.; Wang, W., Acidithiobacillus ferrooxidans and its potential application. *Extremophiles* **2018,** *22* (4), 563-579, DOI 10.1007/s00792-018-1024-9.

42. Ijadi Bajestani, M.; Mousavi, S. M.; Shojaosadati, S. A., Bioleaching of heavy metals from spent household batteries using Acidithiobacillus ferrooxidans: Statistical evaluation and optimization. *Separation and Purification Technology* **2014,** *132*, 309-316, DOI 10.1016/j.seppur.2014.05.023.

43. Mishra, D.; Kim, D. J.; Ralph, D. E.; Ahn, J. G.; Rhee, Y. H., Bioleaching of metals from spent lithium ion secondary batteries using Acidithiobacillus ferrooxidans. *Waste Manag* **2008,** *28* (2), 333-338, DOI 10.1016/j.wasman.2007.01.010.

44. Jegan Roy, J.; Srinivasan, M.; Cao, B., Bioleaching as an Eco-Friendly Approach for Metal Recovery from Spent NMC-Based Lithium-Ion Batteries at a High Pulp Density. *ACS Sustainable Chemistry & Engineering* **2021,** *9* (8), 3060-3069, DOI 10.1021/acssuschemeng.0c06573.

45. Roy, J. J.; Madhavi, S.; Cao, B., Metal extraction from spent lithium-ion batteries (LIBs) at high pulp density by environmentally friendly bioleaching process. *Journal of Cleaner Production* **2021,** *280*, 124242, DOI 10.1016/j.jclepro.2020.124242.

46. Brooks, C. S. In *Selective precipitation of mixed metal hydroxides*, Proceedings of the 45th Industrial Waste Conference May 8, 9, 10, 1990, CRC Press, Boca Raton: 2018; pp 691-696. DOI 10.1201/9781351076036

47. Verma, A.; Kore, R.; Corbin, D. R.; Shiflett, M. B., Metal Recovery Using Oxalate Chemistry: A Technical Review. *Industrial & Engineering Chemistry Research* **2019,** *58* (34), 15381-15393, DOI 10.1021/acs.iecr.9b02598.

48. Zhang, X.; Li, L.; Fan, E.; Xue, Q.; Bian, Y.; Wu, F.; Chen, R., Toward sustainable and systematic recycling of spent rechargeable batteries. *Chem Soc Rev* **2018,** *47* (19), 7239-7302, DOI 10.1039/c8cs00297e.

49. Zhao, Y.; Yuan, X.; Jiang, L.; Wen, J.; Wang, H.; Guan, R.; Zhang, J.; Zeng, G., Regeneration and reutilization of cathode materials from spent lithium-ion batteries. *Chemical Engineering Journal* **2020,** *383*, 123089, DOI 10.1016/j.cej.2019.123089.

50. Or, T.; Gourley, S. W. D.; Kaliyappan, K.; Yu, A.; Chen, Z., Recycling of mixed cathode lithium-ion batteries for electric vehicles: Current status and future outlook. *Carbon Energy* **2020,** *2* (1), 6-43, DOI 10.1002/cey2.29.

51. Natarajan, S.; Aravindan, V., Recycling Strategies for Spent Li-Ion Battery Mixed Cathodes. *ACS Energy Letters* **2018,** *3* (9), 2101-2103, DOI 10.1021/acsenergylett.8b01233.

52. Yadav, P.; Jie, C. J.; Tan, S.; Srinivasan, M., Recycling of cathode from spent lithium iron phosphate batteries. *Journal of Hazardous Materials* **2020,** *399*, 123068, DOI 10.1016/j.jhazmat.2020.123068.

53. Cathode Materials Market by Battery Type (Lead-Acid, Lithium-ion), Material (Lithium-Ion (LFP, LCO, NMC, NCA, LMO), Lead-Acid (Lead Dioxide)), and Region (Asia Pacific, North America, Europe, and Row) - Global Forecast to 2023 https://www.marketsandmarkets.com/Market-Reports/cathode-material-market-246078739.html.

54. Natarajan, S.; Aravindan, V., An Urgent Call to Spent LIB Recycling: Whys and Wherefores for Graphite Recovery. *Advanced Energy Materials* **2020,** *10* (37), 2002238, DOI 10.1002/aenm.202002238.

55. Chen, X.; Ma, H.; Luo, C.; Zhou, T., Recovery of valuable metals from waste cathode materials of spent lithium-ion batteries using mild phosphoric acid. *Journal of Hazardous Materials* **2017,** *326*, 77-86, DOI 10.1016/j.jhazmat.2016.12.021.

56. Fan, X.; Tan, C.; Li, Y.; Chen, Z.; Li, Y.; Huang, Y.; Pan, Q.; Zheng, F.; Wang, H.; Li, Q., A green, efficient, closed-loop direct regeneration technology for reconstructing of the LiNi0.5Co0.2Mn0.3O2 cathode material from spent lithium-ion batteries. *J Hazard Mater* **2021,** *410*, 124610, DOI 10.1016/j.jhazmat.2020.124610.

57. Refly, S.; Floweri, O.; Mayangsari, T. R.; Sumboja, A.; Santosa, S. P.; Ogi, T.; Iskandar, F., Regeneration of LiNi1/3Co1/3Mn1/3O2 Cathode Active Materials from End-of-Life Lithium-Ion Batteries through Ascorbic Acid Leaching and Oxalic Acid Coprecipitation Processes. *ACS Sustainable Chemistry & Engineering* **2020,** *8* (43), 16104-16114, DOI 10.1021/acssuschemeng.0c01006.

58. Zhang, G.; Yuan, X.; He, Y.; Wang, H.; Zhang, T.; Xie, W., Recent advances in pretreating technology for recycling valuable metals from spent lithium-ion batteries. *Journal of Hazardous Materials* **2021,** *406*, 124332, DOI 10.1016/j.jhazmat.2020.124332.

59. Xin, Y.; Guo, X.; Chen, S.; Wang, J.; Wu, F.; Xin, B., Bioleaching of valuable metals Li, Co, Ni and Mn from spent electric vehicle Li-ion batteries for the purpose of recovery. *Journal of Cleaner Production* **2016,** *116*, 249-258, DOI 10.1016/j.jclepro.2016.01.001.

60. Barik, S. P.; Prabaharan, G.; Kumar, L., Leaching and separation of Co and Mn from electrode materials of spent lithium-ion batteries using hydrochloric acid: Laboratory and pilot scale study. *Journal of Cleaner Production* **2017,** *147*, 37-43, DOI 10.1016/j.jclepro.2017.01.095.

61. Gratz, E.; Sa, Q.; Apelian, D.; Wang, Y., A closed loop process for recycling spent lithium ion batteries. *Journal of Power Sources* **2014,** *262*, 255-262, DOI 10.1016/j.jpowsour.2014.03.126.

62. Madhavi, S.; Subba Rao, G. V.; Chowdari, B. V. R.; Li, S. F. Y., Effect of aluminium doping on cathodic behaviour of LiNi0.7Co0.3O2. *Journal of Power Sources* **2001,** *93* (1), 156-162, DOI 10.1016/S0378-7753(00)00559-0.

63. Chen, C. H.; Liu, J.; Stoll, M. E.; Henriksen, G.; Vissers, D. R.; Amine, K., Aluminum-doped lithium nickel cobalt oxide electrodes for high-power lithium-ion batteries. *Journal of Power Sources* **2004,** *128* (2), 278-285, DOI 10.1016/j.jpowsour.2003.10.009.

64. Chen, X.; Xu, B.; Zhou, T.; Liu, D.; Hu, H.; Fan, S., Separation and recovery of metal values from leaching liquor of mixed-type of spent lithium-ion batteries. *Separation and Purification Technology* **2015,** *144*, 197-205, DOI 10.1016/j.seppur.2015.02.006.

65. Habibi, A.; Jalaly, M.; Rahmanifard, R.; Ghorbanzadeh, M., The effect of calcination conditions on the crystal growth and battery performance of nanocrystalline Li(Ni1/3Co1/3Mn1/3)O2 as a cathode material for Li-ion batteries. *New Journal of Chemistry* **2018,** *42* (23), 19026-19033, DOI 10.1039/C8NJ05007D.

66. Yao, X.; Xu, Z.; Yao, Z.; Cheng, W.; Gao, H.; Zhao, Q.; Li, J.; Zhou, A., Oxalate co-precipitation synthesis of LiNi0.6Co0.2Mn0.2O2 for low-cost and high-energy lithium-ion batteries. *Materials Today Communications* **2019,** *19*, 262-270, DOI 10.1016/j.mtcomm.2019.02.001.

For Table of Contents Use Only

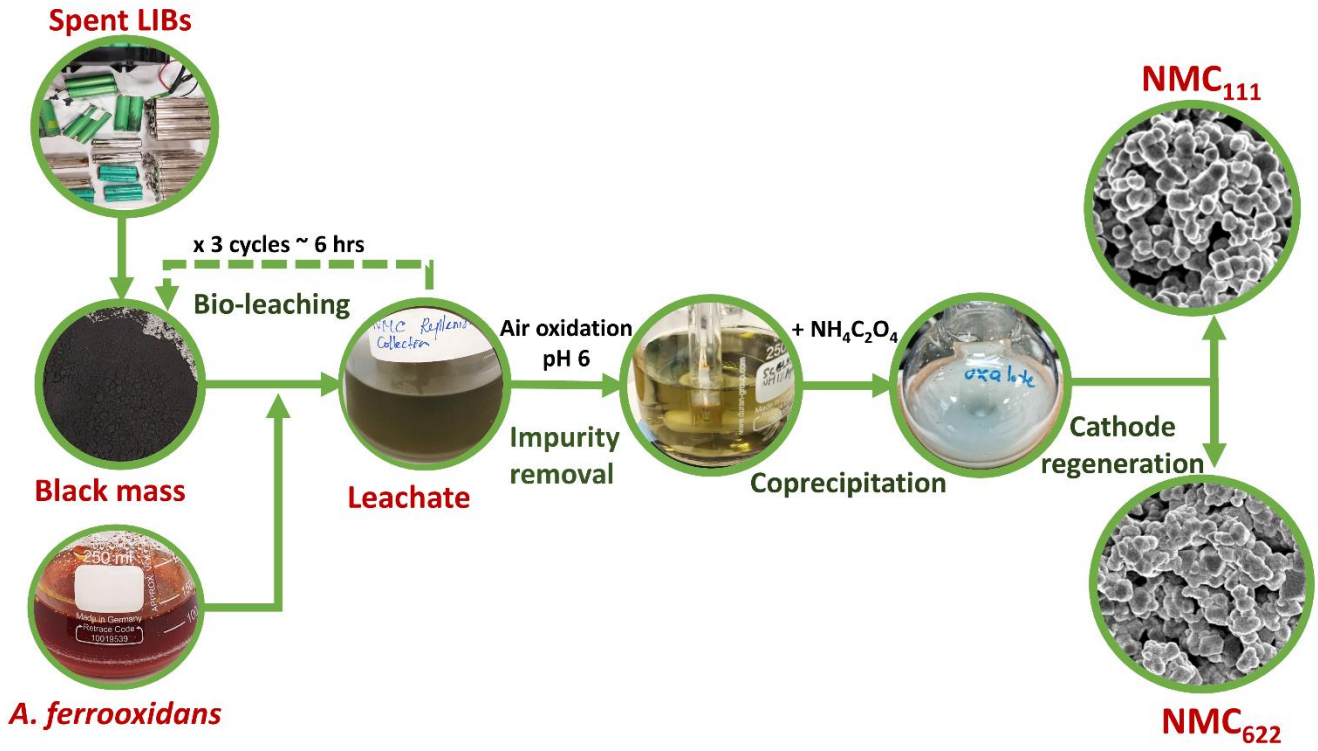

A sustainable process for recycling cathode material $LiMn_XNi_yCo_{1-x-y}O_2$ from spent lithium-ion batteries through *Acidithiobacillus ferrooxidan* mediated bioleaching

Supporting Information

Green closed-loop cathode regeneration from spent NMC-based lithium-ion batteries through bioleaching

Minh Phuong Do [#] [†,‡], Joseph Jegan Roy [#] [†,‖,‡], Bin Cao* [‖,§], Madhavi Srinivasan ** [†, ‡]

[†] Energy Research Institute @ NTU (ERI@N), SCARCE Laboratory, Nanyang Technological University, 62 Nanyang Dr, Singapore 637459

[‖] Singapore Centre for Environmental Life Sciences Engineering, Nanyang Technological University, 60 Nanyang Dr, Singapore 637551

[‡] School of Materials Science and Engineering, Nanyang Technological University, 50 Nanyang Avenue, Singapore 639798

[§] School of Civil and Environmental Engineering, Nanyang Technological University, 50 Nanyang Avenue, Singapore 639798

[#] These author has equally contributed to this work

* Corresponding Authors

Contact: BinCao@ntu.edu.sg Tel.: +65 67905277
Madhavi@ntu.edu.sg Tel.: +65 67904606
jeganroy@ntu.edu.sg
minhphuong.do@ntu.edu.sg

Number of pages: 7

Number of tables: 1

Number of figures: 8

Table S1. The metal concentration of leachate after progressive precipitation without aeration

Metals	NMC Source soln pH 2.5 ppm	1st Pption pH 3.0 ppm	2nd Pption pH 4.0 ppm	3rd Pption pH 4.8 ppm	4th Pption pH 5.0 ppm
Ni	4364.75	4294.65	4016.86	3907.19	4021.92
Mn	2670.33	2625.49	2502.87	2634.62	2578.89
Co	2111.08	2066.01	1945.02	1893.41	1853.65
Li	1116.09	1131.72	1130.62	1092.18	1178.22
Cu	531.63	546.45	309.84	76.30	NA
Al	75.82	89.39	79.83	63.69	52.27
Fe	11869.26	11152.67	9044.12	8347.54	8477.03

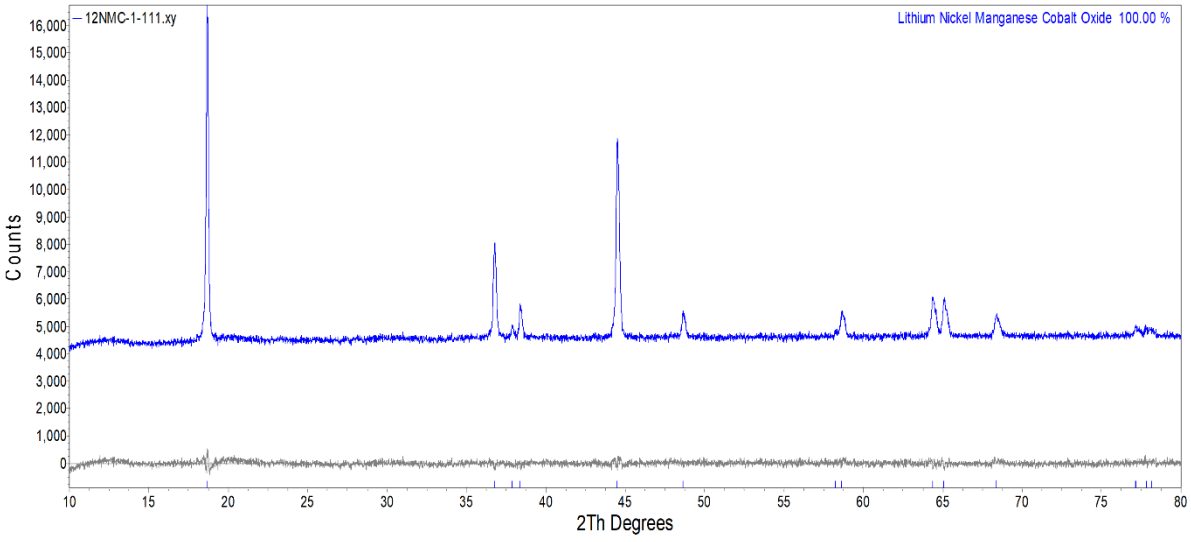


```
Rexp : 1.46    Rwp : 1.70    Rp  : 1.34   GOF : 1.17
Rexp`: 8.82    Rwp`: 10.31   Rp` : 10.59  DW  : 1.49
```

Figure S1. XRD refinement of NMC_{111} (900 °C)

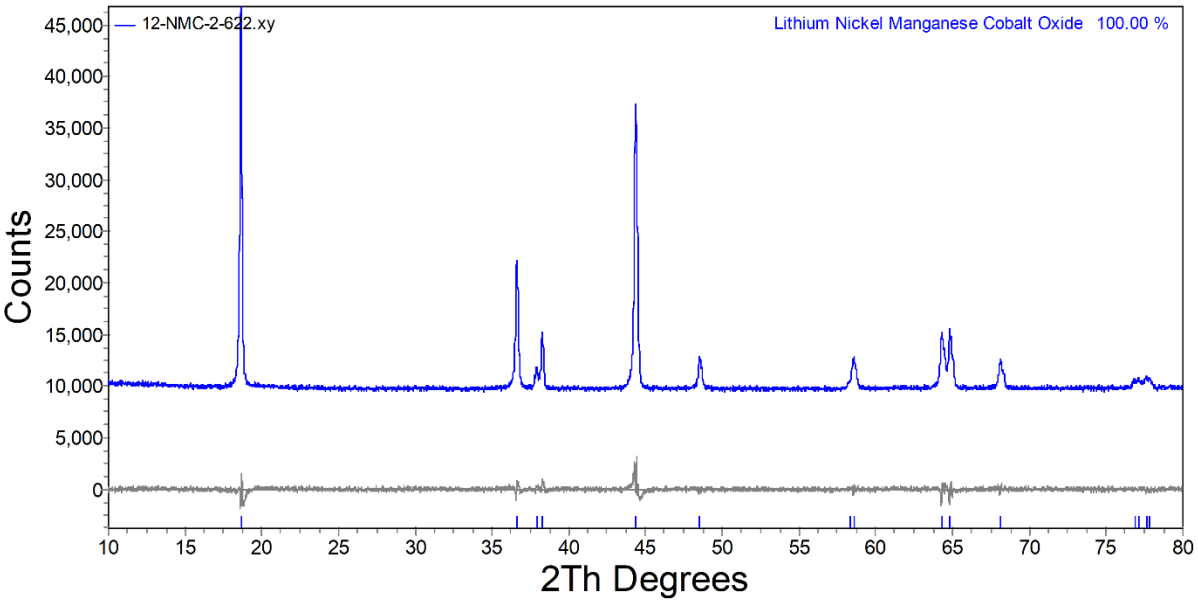

Rexp : 0.99	Rwp : 1.74	Rp : 1.16	GOF : 1.76
Rexp`: 6.89	Rwp`: 12.15	Rp` : 15.28	DW : 0.81

Figure S2. XRD refinement of NMC_{622} (850 °C)

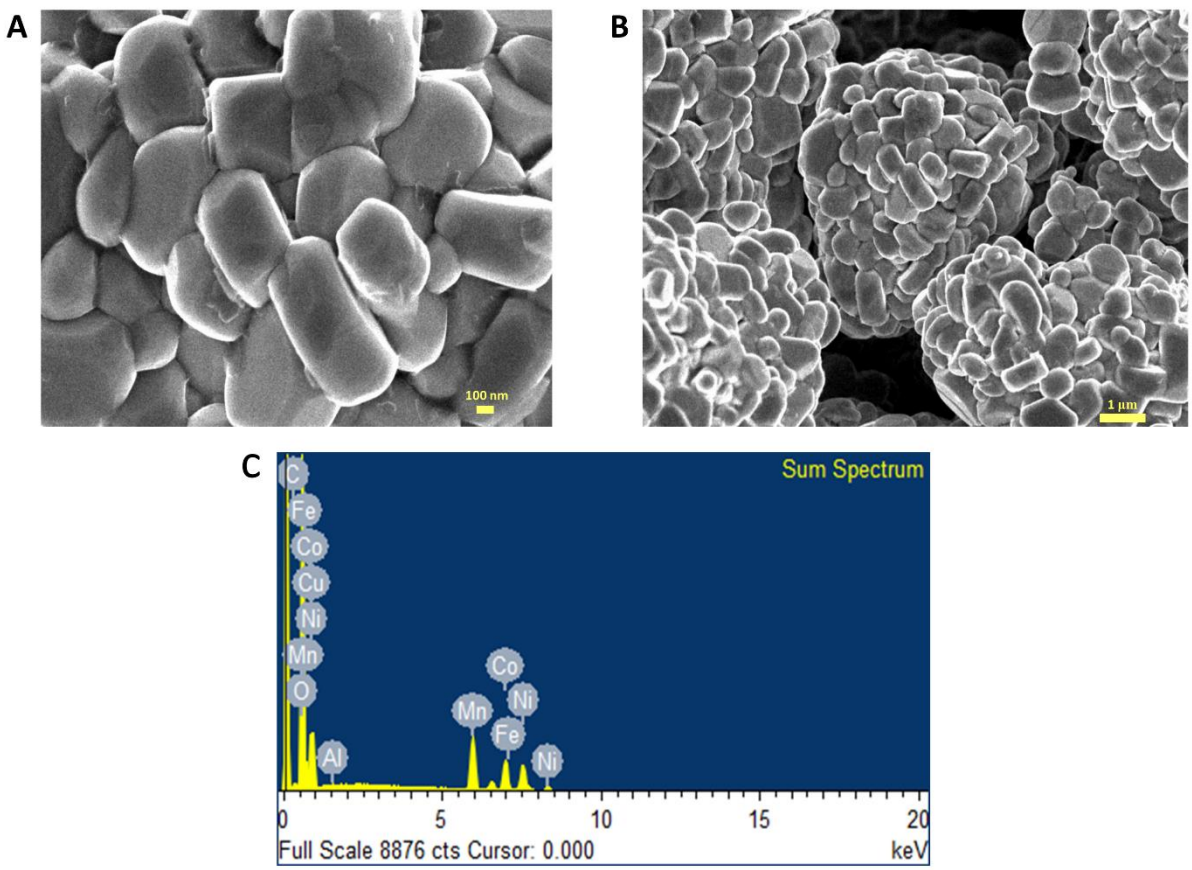

Figure S3. (A and B) SEM images and (C) EDX of commercial NMC (ENAX)

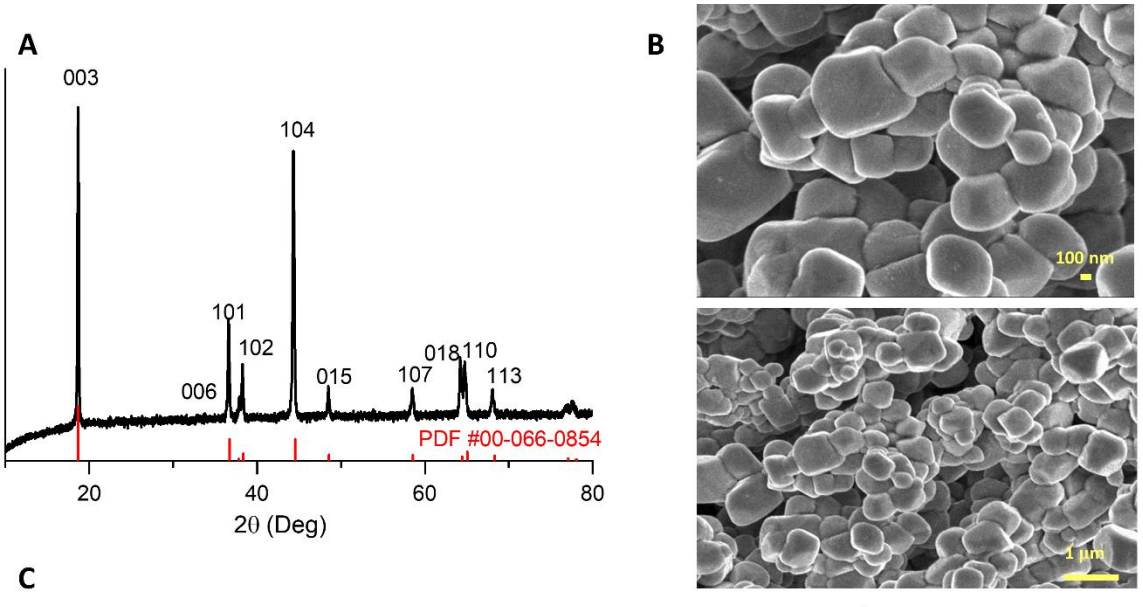

C

Cathode material	a	c	c/a	I(003)/I(104)
NMC $_{622}$-900 °C	2.878768	14.257617	4.952661	1.108

Figure S4. (A) XRD pattern (B) SEM images (C) Refined lattice parameter, lattice parameter ratio, and peak intensity ratio of (003) and (104) of NMC$_{622}$ annealing at 900 °C

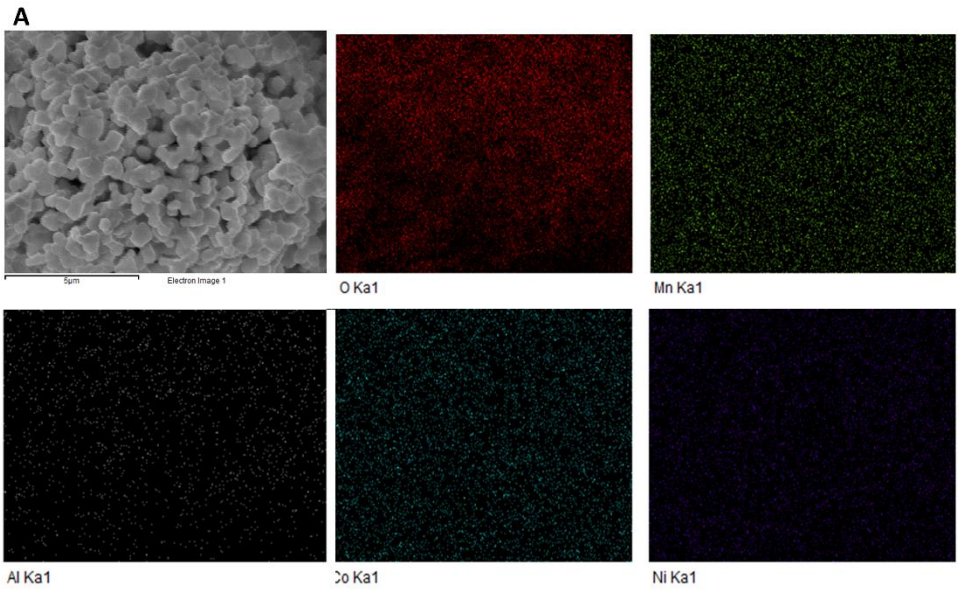

B

Element	% Weight	% Atomic
O	38.94	69.44
Al	0.57	0.60
Mn	18.16	9.43
Co	20.34	9.85
Ni	21.98	10.68
Total	100.00	100.00

Figure S5 (A) EDX mapping of recycled NMC$_{111}$, (B) Elemental composition from EDX spectra

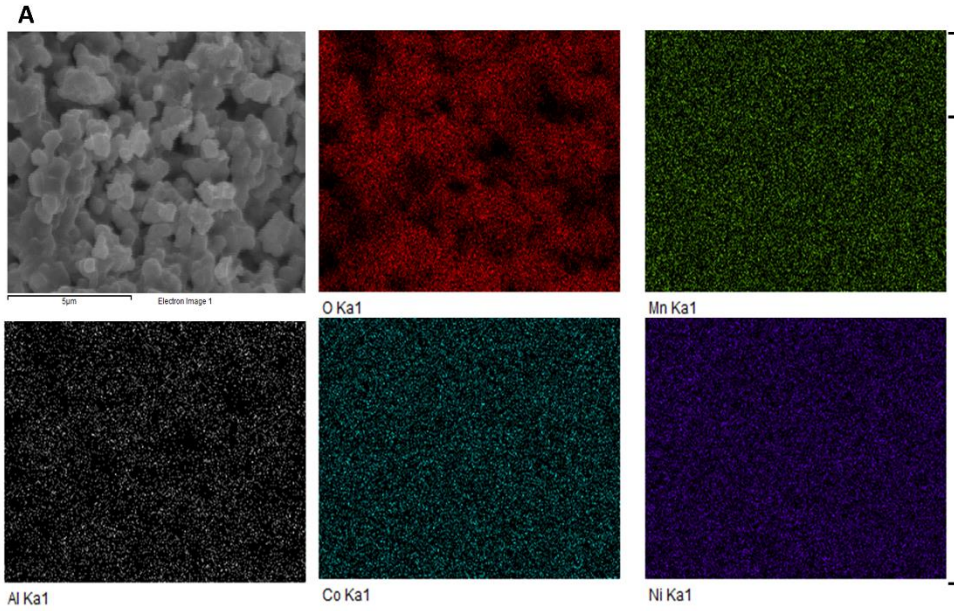

B

Element	% Weight	% Atomic
O	38.18	69.03
Al	0.22	0.24
Mn	12.34	6.50
Co	13.14	6.45
Ni	36.11	17.79
Total	100.00	100.00

Figure S6 (A) EDX mapping of recycled NMC_{622}, (B) Elemental composition from EDX spectra

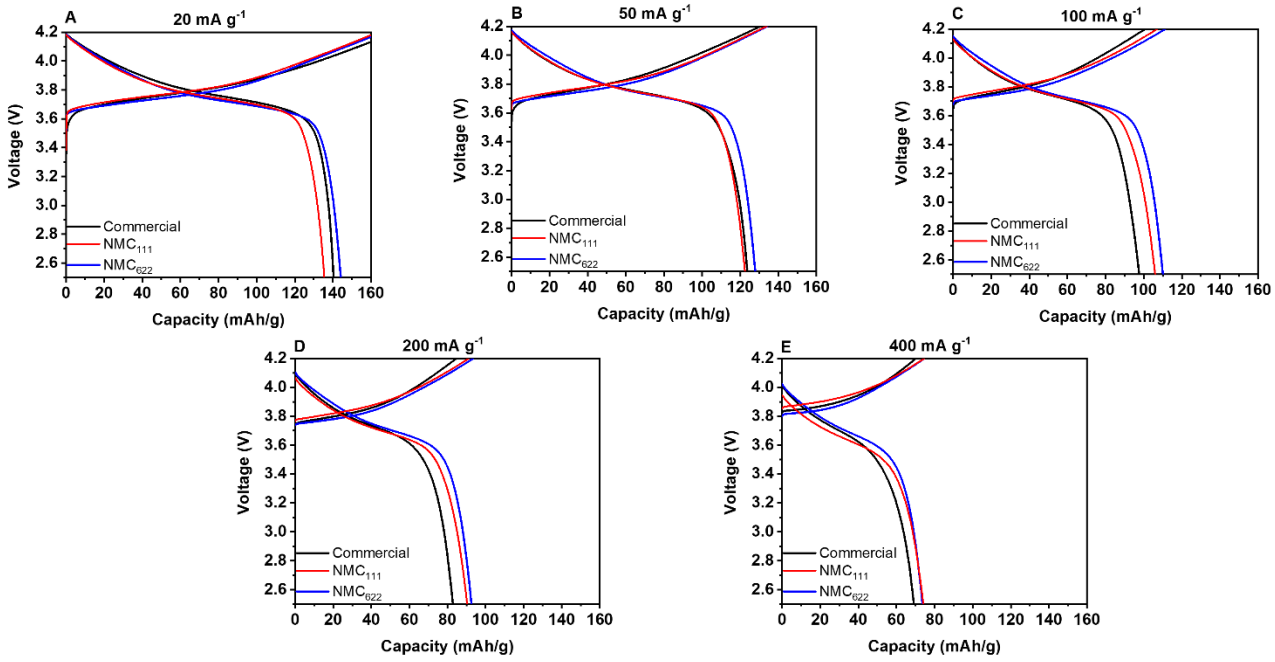

Figure S7. (A-E) Galvanostatic charge-discharge curves comparison between recycled NMC_{111}, NMC_{622}, and NMC commercial at 20 mA g^{-1} (A), 50 mA g^{-1} (B), 100 mA g^{-1} (C), 200 mA g^{-1} (D) and 400 mA g^{-1} (E) in the voltage range from 2.5 to 4.2 V vs Li/Li^+

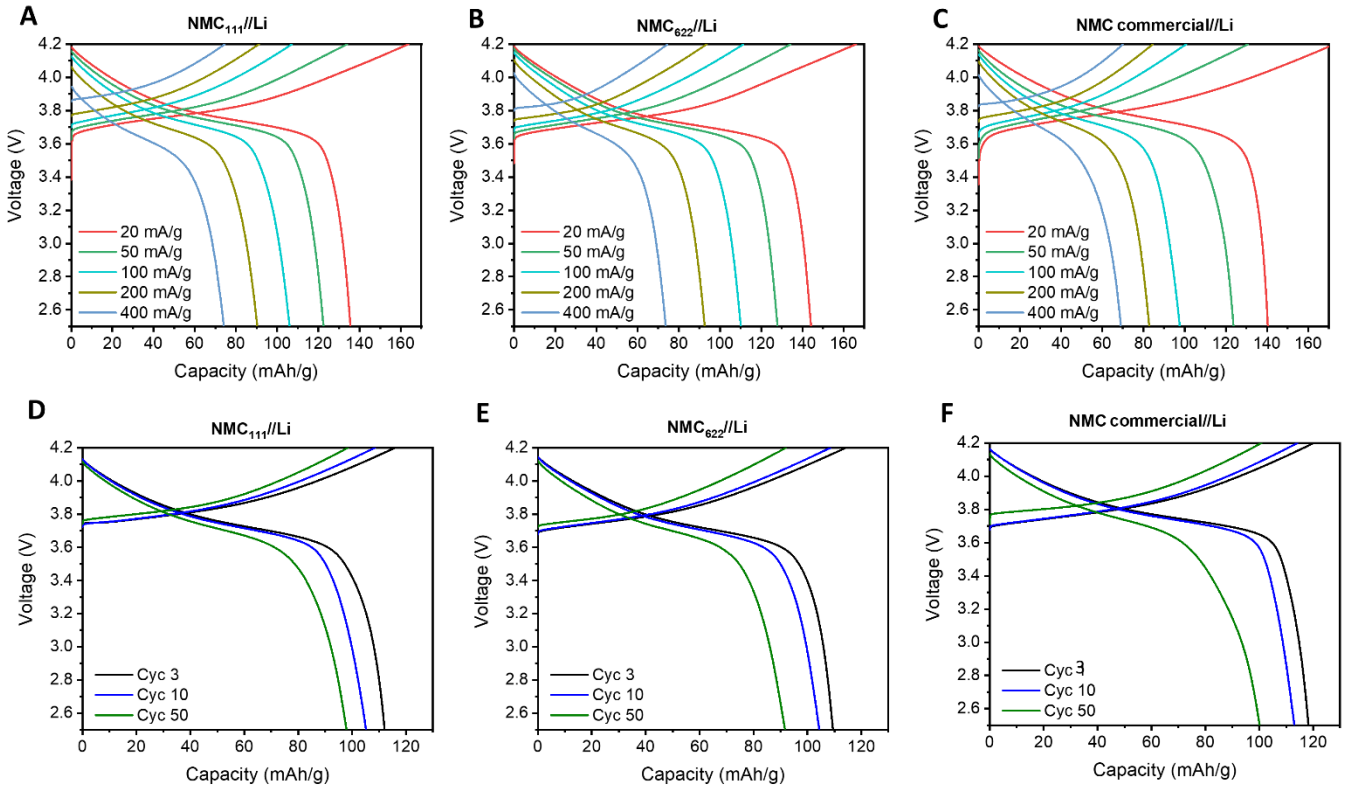

Figure S8. Galvanostatic charge-discharge curves of recycled NMC_{111} (A, D), NMC_{622} (B, E), and NMC commercial (C, F); half cell at different current rates (A, B, C) and in different cycle numbers (D, E, F) in the voltage range from 2.5 to 4.2 V vs Li/Li^+